This authors' personal copy may not be publicly or systematically copied or distributed, or posted on the Open Web, except with written permission of the copyright holder(s). It may be distributed to interested individuals on request.

Vol. 578: 51–72, 2017
https://doi.org/10.3354/meps12229

MARINE ECOLOGY PROGRESS SERIES
Mar Ecol Prog Ser

Published August 31

Seasonality in the vertical flux and species composition of Radiolaria Polycystina (Protista): patterns and drivers

Demetrio Boltovskoy*

Instituto de Ecología, Genética y Evolución de Buenos Aires (IEGEBA-CONICET), Facultad de Ciencias Exactas y Naturales, Universidad de Buenos Aires, 1428 Buenos Aires, Argentina

ABSTRACT: Radiolarian flux rates, their intermittency, and changes in their species compositions are assessed using data from 73 time series sediment trap deployments (1357 samples) covering 7 to 12 calendar months. Results are analyzed as a function of trap depth, latitude, and seasonal and geographic variations in sea surface temperature and primary production. Radiolarian flux rates are highest in the tropics and subtropics, decreasing towards the high latitudes. Low and highly intermittent primary production (PP) regimes are reflected in more pulsating radiolarian flux rates, but in moderate to high PP areas, radiolarian fluxes are not associated with phytoplanktonic growth cycles. At sites where simultaneous trap deployments at different depths were performed, shallower traps yield lower and more pulsating radiolarian flux values than deeper ones. Enhanced dissolution of biogenic silica in the shallower traps is probably responsible for these differences. Intermittency in radiolarian flux is highest in the seasonally ice-covered Southern Ocean waters, but much lower in the also seasonally ice-covered northern hemisphere sites investigated, suggesting differences in the mechanisms that govern the production and recycling of organic matter in the upper ocean and at mid depths. Radiolarian flux rates and their species richness do not seem to be coupled, either temporally or geographically. Temporal stability in the composition of the radiolarian taxocoenoses is generally high, and positively associated with absolute flux values and trap depth. The bulk of the assemblages are little affected by environmental seasonality, and only a few species, albeit often numerically dominant, seem to reflect these changes.

KEY WORDS: Radiolarian · Polycystinea · Seasonality · Vertical flux · Sediment traps · World Ocean · Species composition

Resale or republication not permitted without written consent of the publisher

INTRODUCTION

Polycystine Radiolaria (Rhizaria, Retaria, Polycystinea, according to the recent phylogenetic classification scheme of Adl et al. 2012) are an important component of the marine, open-ocean protozooplankton, and one of the few with an extensive fossil record (De Wever et al. 2001). In spite of major problems in their generic and infrageneric classification (Lazarus et al. 2015), the worldwide distribution patterns of a significant fraction of the extant radiolarians have been reasonably well defined (Nigrini 1967, Petrushevskaya 1971a, Strelkov & Reshetnjak 1971, Moore 1978, Nigrini & Moore 1979, Pisias et al. 1997, Cortese et al. 2003, Boltovskoy et al. 2010, Boltovskoy & Correa 2016). While these distributional data are fundamental for describing the environmental envelopes of the species, our understanding of radiolarian ecology is still very limited. A major gap in our knowledge concerns the effects of seasonality on radiolarian abundance and species compositions. Such knowledge should ideally be derived from analyses of seasonal plankton collections, but such collections have very seldom been conducted, and

*Corresponding author: boltovskoy@gmail.com

© Inter-Research 2017 · www.int-res.com

Author copy

their geographic and/or bathymetric coverage has been limited (e.g. Bjørklund 1972, Boltovskoy & Riedel 1987).

An alternative to plankton materials are time series sediment trap samples. Sediment trap samples have the advantage of covering entire annual cycles, often at monthly or even higher time resolutions. Further, time series trap deployments have been performed in many different locations with widely contrasting environmental conditions, making them amenable to searching cause–effect relationships applicable on large geographic scales (Lampitt & Antia 1997, Lutz et al. 2007, Lima et al. 2014). However, in radiolarian studies, attempts at deriving general trends from these reports have been very limited (e.g. Suzuki & Not 2015).

The analyses presented in this work are aimed at addressing the following questions: (1) What drives radiolarian vertical flux rates, and what are the confounding factors that affect the figures reported? (2) What factors are associated with the intermittency (seasonality) of radiolarian flux rates? (3) How are flux rates and their intermittency associated with seasonal changes in the specific composition of the settling assemblages? The results contribute towards the interpretation of the environmental drivers that affect sediment trap collections, and the use of radiolarians for biogeographic and paleoecological surveys based on water column and surface sediment materials.

MATERIALS AND METHODS

Data used for this work were compiled from 16 publications which reported time series radiolarian flux rates over periods of approximately 1 yr at 32 sites throughout the World Ocean. Several trap deployments had longer durations (up to 15 yr); in these cases, only the samples that spanned 1 or more consecutive calendar years were included. These were treated as separate series (rather than pooled), whereas the rest of the samples (covering a few months before and/or after the time offsets used) were discarded. Consecutive time offsets of the same trap deployment and depth were considered separately because interannual variations in flux rates can be very marked, often in association with El Niño versus La Niña conditions (e.g. Takahashi 1987, 1997, Ikenoue et al. 2012a, 2015).

The core set of data are 40 time-series deployments conducted between 1983 and 2003 (10 to 26 samples per series, 823 samples in total) for which radiolarian flux rates and species identifications were provided in the original sources, as compiled by Boltovskoy et al. (2010) (Table 1; henceforth referred to as 'Dataset 1'). These series covered 280 to 402 consecutive days over 11 to 12 calendar months (with the exception of 1 series, which covered 10 mo) (Fig. 1).

Several important surveys were not included in the analyses of the temporal changes in specific radiolarian compositions because they did not provide lists of all the species recorded in their samples (e.g. Takahashi 1987, 1997, Gowing 1993, Lange et al. 1997, Romero et al. 2001, Hays & Morley 2003, Motoyama et al. 2005, Ikenoue et al. 2012a), or because their taxonomic framework differed considerably from the one adopted for all other reports (e.g. Ikenoue et al. 2015), which was the result of a team work (Boltovskoy et al. 2010). This information (henceforth referred to as 'Dataset 2'), which was included in the estimates of radiolarian flux and seasonality, consists of 33 deployments (9 to 31 samples per series, 581 samples in total, 1982 to 2012) (Table 2, Fig. 1). Dataset 2 included 4 series which covered 7 to 9 mo only (series 101 to 105 in Table 2), and 1 series that was non-continuous (series 106). Despite their limitations, these series were included in assessments of seasonal variations in radiolarian flux because they were performed in mid-latitude areas, poorly represented in the literature.

Most (92%) of the samples used were sieved with 0.040 to 0.063 mm meshes before counting, but 1 series used a 0.015 mm sieve (series 21), and 7 series (25, 101 to 106) used unsieved materials (Tables 1 & 2). Radiolarian flux rates in these collections are probably more realistic, but only marginally comparable to the flux rates reported by the other surveys (see 'Discussion: Limitations and caveats'). Results which might have been biased by these methodological differences are explicitly addressed throughout the text and excluded from the analyses or treated separately.

Sea surface temperature (SST) data are from Boyer et al. (2013) (1955 to 2012), whereas primary productivity (PP) data are from the Ocean Productivity database (www.science.oregonstate.edu/ocean.productivity/, 1997 to 2012).

For assessing the intermittency in primary production and radiolarian flux, the 'production half-time' concept proposed by Berger & Wefer (1990) was used, defined as the length of time it takes to generate half of the annual productivity, when the data are ordered from highest to lowest. Thus, shorter time intervals to reach 50% of the total yearly flux (or primary production) are indicative of a more pulsed out-

Author copy

Table 1. Dataset 1. General information on the sediment trap series with detailed taxonomic information. Sources of data: Series 1 to 3: Abelmann (1992); 4, 5, 19, 20, 22 to 24: Takahashi & Yamashita (2004); 6 to 18: Okazaki et al. (2008); 21: Boltovskoy et al. (1993); 25: Boltovskoy et al. (1996); 26 to 28, 31, 32: Okazaki et al. (2005); 29, 30, 33, 34: Okazaki et al. (2003); 35 to 40: Schröder-Ritzrau (1995). PP: primary production (PP half-time = Time to generate half of the productivity of the entire period considered when daily data are ordered from highest to lowest); MRF: mean radiolarian flux; RFS: radiolarian flux stability (= Time to generate half of the flux of the entire period considered when daily data are ordered from highest to lowest); RSCS: radiolarian specific composition stability; SD: standard deviation; SST: sea surface temperature

Trap series code no.	Lat.	Long.	Trap depth (m)	Duration (mo)	No. of samples	Sieve mesh size (mm)	SST annual mean (span) (°C)	PP annual mean (span) (gC m^{-2} yr^{-1})	PP half-time (d)	MRF (ind. m^{-2} d^{-1})	RFS (d)	Species recorded Total[a]	Species recorded In >50% of months[b]	Mean (SD) RSCS Morisita	Mean (SD) RSCS Ochiai	PP vs. rad. flux, Spearman's R (p)
1	−62.34	−57.31	693	11	12	0.040	2.6 (2.8)	171 (315)	22.1	37	2.7	17	11.8	0.344 (0.316)	0.333 (0.300)	0.726 (0.006)
2	−62.26	−57.53	494	12	10	0.040	−0.6 (3.3)	179 (733)	14.8	763	7.6	12	8.3	0.367 (0.374)	0.408 (0.334)	0.846 (0.001)
3	−62.26	−57.53	1588	12	11	0.040	−0.5 (3.3)	195 (733)	16.0	5870	6.1	10	10.0	0.418 (0.403)	0.491 (0.289)	0.385 (0.237)
4	−0.01	145.02	1020	11	22	0.063	29.3 (0.6)	283 (93)	44.9	4782	16.8	130	42.3	0.528 (0.222)	0.505 (0.123)	0.709 (0.000)
5	−0.01	145.02	2060	11	22	0.063	29.3 (0.6)	283 (93)	44.9	6538	30.6	146	63.7	0.799 (0.134)	0.653 (0.122)	0.646 (0.001)
6	0.00	145.00	2030	12	26	0.063	29.3 (0.6)	282 (93)	45.5	6861	24.7	102	54.9	0.532 (0.257)	0.483 (0.212)	0.519 (0.006)
7	0.00	145.00	1960	12	24	0.063	29.3 (0.6)	283 (93)	45.1	8166	31.5	127	67.7	0.769 (0.070)	0.678 (0.059)	0.108 (0.615)
8	0.00	145.00	1962	10	19	0.063	29.4 (0.6)	271 (78)	46.4	8948	29.7	118	61.9	0.741 (0.225)	0.560 (0.166)	−0.197 (0.418)
9	0.00	160.00	1990	12	26	0.063	29.4 (0.4)	218 (60)	46.7	9597	21.9	95	63.2	0.669 (0.180)	0.591 (0.160)	0.741 (0.000)
10	0.00	160.00	2070	12	25	0.063	29.4 (0.4)	220 (60)	46.5	10160	28.8	126	65.1	0.803 (0.070)	0.700 (0.056)	0.116 (0.580)
11	0.00	175.00	3000	11	21	0.063	28.7 (1.1)	295 (86)	45.5	14761	28.0	114	69.3	0.778 (0.103)	0.691 (0.079)	0.153 (0.506)
12	0.00	175.00	2970	12	26	0.063	28.7 (1.1)	296 (86)	46.0	17987	26.4	105	69.5	0.811 (0.140)	0.694 (0.139)	0.555 (0.003)
13	0.00	175.00	3090	12	25	0.063	28.7 (1.1)	296 (86)	45.8	17425	30.3	121	72.7	0.853 (0.113)	0.735 (0.108)	0.677 (0.000)
14	0.00	175.00	3090	12	23	0.063	28.7 (1.1)	296 (86)	45.7	16027	33.2	126	65.1	0.878 (0.086)	0.686 (0.088)	0.397 (0.059)
15	0.00	−170.00	3040	11	21	0.063	27.9 (1.2)	341 (52)	48.1	23950	36.8	99	53.5	0.813 (0.063)	0.684 (0.049)	0.441 (0.044)
16	0.00	−170.00	2850	12	24	0.063	28.0 (1.2)	338 (59)	48.2	23282	31.9	125	80.8	0.856 (0.178)	0.698 (0.154)	0.459 (0.023)
17	0.00	−160.00	3120	12	24	0.063	27.4 (1.2)	368 (47)	48.4	15588	32.6	122	73.8	0.878 (0.060)	0.722 (0.079)	0.176 (0.410)
18	0.00	−160.00	3070	12	25	0.063	27.3 (1.2)	368 (47)	48.2	23087	32.1	129	77.5	0.864 (0.116)	0.662 (0.147)	0.231 (0.265)
19	0.02	174.56	1040	11	22	0.063	28.7 (1.1)	295 (87)	45.7	5560	26.0	141	44.7	0.704 (0.110)	0.588 (0.072)	0.100 (0.658)
20	0.02	174.56	3000	11	21	0.063	28.7 (1.1)	293 (87)	45.5	14755	28.0	148	65.5	0.821 (0.090)	0.684 (0.077)	0.153 (0.506)
21	1.79	−11.13	853	12	20	0.015	27.2 (4.1)	476 (449)	38.1	28466	27.4	143	61.5	0.954 (0.033)	0.670 (0.057)	−0.433 (0.055)
22	4.02	135.00	970	11	22	0.063	29.0 (1.2)	260 (61)	47.4	12303	24.7	132	48.5	0.774 (0.091)	0.643 (0.070)	0.575 (0.005)
23	4.02	135.00	2940	11	22	0.063	29.1 (1.2)	259 (61)	47.4	13947	34.6	139	58.3	0.768 (0.131)	0.649 (0.105)	0.768 (0.000)
24	5.04	140.06	2970	11	22	0.063	29.1 (0.9)	204 (67)	45.8	13197	22.7	134	64.2	0.780 (0.119)	0.670 (0.095)	0.519 (0.013)
25	20.92	−19.74	2195	11	13	0.000	21.8 (4.6)	706 (558)	40.3	78325	36.5	106	38.7	0.975 (0.019)	0.605 (0.076)	−0.177 (0.561)
26	40.00	165.00	2986	12	22	0.063	14.2 (10.4)	551 (455)	38.8	10725	37.8	110	78.2	0.644 (0.220)	0.803 (0.046)	−0.002 (0.992)
27	43.97	155.05	2957	12	21	0.063	7.9 (12.4)	525 (752)	30.6	6178	41.2	78	75.6	0.779 (0.102)	0.728 (0.051)	0.331 (0.142)
28	43.97	155.05	2957	12	22	0.063	7.6 (12.4)	543 (752)	31.5	6195	38.8	78	71.8	0.770 (0.107)	0.716 (0.057)	−0.022 (0.922)
29	49.50	146.47	300	11	18	0.063	3.4 (13.2)	764 (1418)	28.1	209	20.6	17	23.5	0.267 (0.289)	0.291 (0.294)	0.429 (0.074)
30	49.50	146.47	700	11	20	0.063	3.0 (13.2)	708 (1418)	27.5	750	18.5	33	27.3	0.684 (0.175)	0.544 (0.146)	0.578 (0.007)
31	50.02	165.03	3260	11	19	0.063	5.1 (9.0)	404 (745)	28.1	4580	36.2	73	58.9	0.829 (0.181)	0.690 (0.174)	0.111 (0.650)
32	50.02	165.03	3260	12	21	0.063	5.0 (9.0)	424 (745)	28.6	3803	37.5	73	56.2	0.856 (0.072)	0.698 (0.050)	−0.335 (0.136)
33	53.02	145.50	300	11	17	0.063	3.8 (14.2)	982 (1824)	25.6	409	13.4	22	18.2	0.272 (0.248)	0.327 (0.231)	0.443 (0.072)
34	53.02	145.50	1550	11	21	0.063	3.3 (14.2)	858 (1824)	25.6	2013	24.6	44	29.5	0.768 (0.161)	0.689 (0.095)	0.027 (0.908)
35	69.69	−0.46	1000	12	20	0.045	6.0 (5.3)	493 (1099)	20.8	3449	17.9	37	56.8	0.915 (0.066)	0.697 (0.079)	0.053 (0.825)
36	69.69	−0.46	3000	12	20	0.045	6.0 (5.3)	493 (1099)	20.8	27748	38.1	36	75.0	0.965 (0.017)	0.826 (0.051)	−0.326 (0.158)
37	72.01	−7.04	500	11	17	0.045	1.9 (6.0)	414 (1099)	21.9	2330	15.9	23	43.5	0.850 (0.111)	0.679 (0.139)	0.120 (0.645)
38	72.01	−7.04	1000	11	19	0.045	2.3 (6.0)	469 (1099)	23.1	3543	19.4	28	67.9	0.894 (0.086)	0.746 (0.125)	0.000 (1.000)
39	72.38	−7.71	1000	12	19	0.045	1.7 (5.9)	481 (1099)	19.7	2290	14.5	31	58.1	0.837 (0.099)	0.765 (0.068)	0.030 (0.903)
40	72.38	−7.71	2300	12	19	0.045	1.7 (5.9)	481 (1099)	19.7	5709	38.1	26	76.9	0.908 (0.074)	0.854 (0.051)	−0.363 (0.124)

[a]As compiled by Boltovskoy et al. (2010); [b]As a percentage of all species recorded in the entire series

Author copy

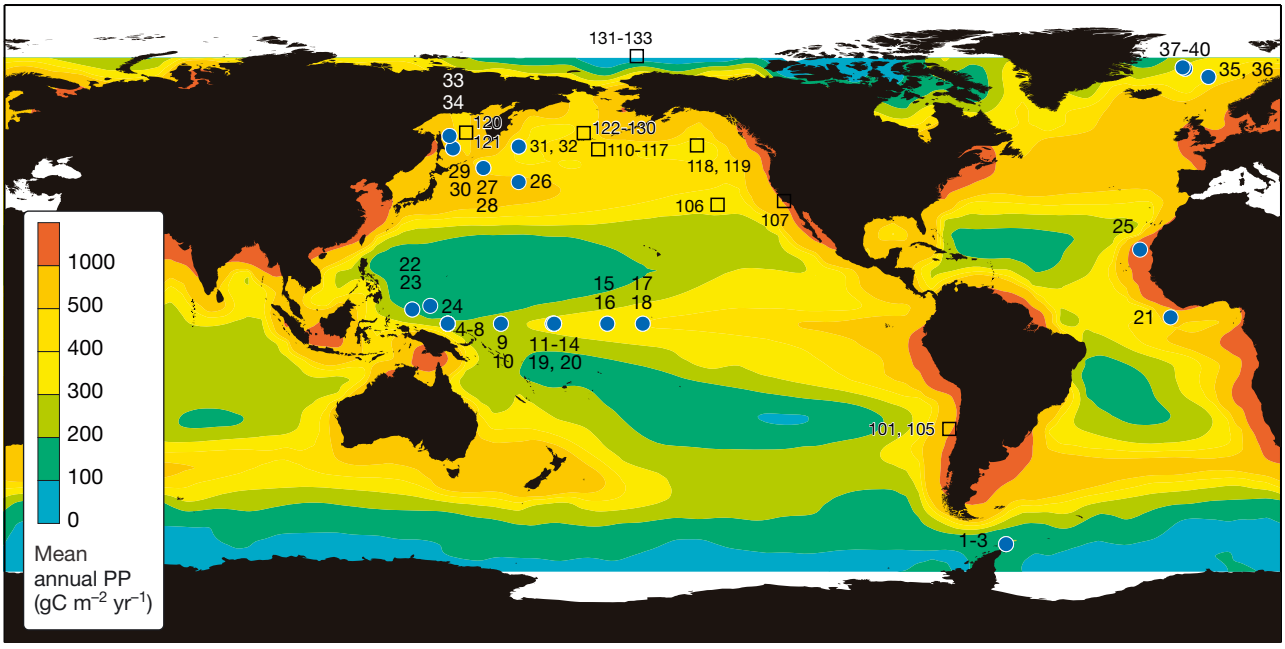


Fig. 1. Geographic distribution of the sediment trap series investigated, and mean annual primary production (PP) values. (●) Series for which detailed taxonomic information was available (Dataset 1); (□) series with information on radiolarian flux rates only (Dataset 2). Refer to Tables 1 & 2 for sources

put and stronger seasonality, whereas longer ones signify a more even distribution of production or flux throughout the year and less marked seasonality.

Because trapping periods differed in extension and periodicity, rather than using months as the base time unit, the daily values for each series were interpolated linearly using the reported collecting cup opening and closing dates, sorted in decreasing order, and the number of days necessary to reach a given proportion of the overall flux for the entire series was calculated. To account for the effects of different trapping periods, times to reach 50% of the total flux were expressed as a proportion of the overall trapping time of each deployment, henceforth referred to as the radiolarian flux stability (RFS). RFS values were not affected by differences in trap deployment periods (Pearson's R = 0.172, p = 0.144; log-transformed data). A potential pitfall of this method is that flux values between consecutive samples may not have followed a linear trend, but this problem also affects calculations based on months (where 1 or 2 values are extrapolated over 30 d periods), and since the sampling interval of most of the trap series used was less than a month (mean for the 73 series: 16 d), it still reflects temporal changes in flux rates more accurately. A similar approach was used for calculating primary production half-times on the basis of mean monthly values for 1997 to 2012, where months were defined using the mid-day of each trapping interval of each series.

A preliminary assessment of the changes in the radiolarian composition in the traps throughout the year was performed by means of 2 faunal similarity indices widely used in ecological surveys: Ochiai's binary (presence–absence) index and Morisita's quantitative index (based on percentages). Both indices have been found to behave consistently under a wide range of conditions (Wolda 1981, Hubálek 1982, Bolton 1991), but their results are not always coincident (Boltovskoy & Correa 2016). However, in our data mean similarities between all the samples of each series (radiolarian specific composition stability, RSCS) measured with the binary (Ochiai) and the quantitative (Morisita) indices were similar and very highly significantly correlated (Fig. 2), suggesting that, at the scale of these analyses, the information conveyed by species presence–absence data is closely comparable to that based on species proportions. Relying on this tight coupling, only the quantitative (Morisita) similarity index was used in all subsequent analyses.

For each of the sediment trap series considered, the faunal similarity indices for every pair of samples were calculated and the resulting mean RSCS value, and its standard deviation (RSCS SD), were used.

Author copy

Table 2. Dataset 2. General information on the sediment trap series without detailed taxonomic information. Sources of data: Series 101 to 105: Romero et al. (2001); 106: Gowing (1993); 107: Lange et al. (1997); 108 to 117, 122 to 130: Ikenoue et al. (2012a); 118, 119: Takahashi (1987); 120, 121: Hays & Morley (2003); 131 to 133: Ikenoue et al. (2015). See Table 1 for notes and abbreviations

Trap series code no.	Lat.	Long.	Trap depth (m)	Duration (mo)	Total no. of samples	Sieve mesh size (mm)	SST annual mean (span) (°C)	PP annual mean (span) (gC m^{-2} yr^{-1})	PP half-time (d)	MRF (ind. m^{-2} d^{-1})	RFS (d)	PP vs. rad. flux, Spearman's R (p)
101	−30.05	−73.17	2303	7	20	–	15.9 (5.0)	707.1 (258.1)	47.2	2345	34.2	0.227 (0.335)
102	−30.03	−73.18	2333	7	20	–	15.9 (5.0)	707.1 (258.1)	46.1	13470	28.3	−0.304 (0.191)
103	−30.00	−73.28	1492	8	17	–	15.9 (5.0)	707.1 (258.1)	46.1	6382	23.0	0.570 (0.016)
104	−30.00	−73.28	2578	9	20	–	15.9 (5.0)	707.1 (258.1)	46.5	6195	15.2	−0.024 (0.921)
105	−29.98	−73.30	2526	8	19	–	15.9 (5.0)	707.1 (258.1)	44.9	4253	24.4	0.763 (0.000)
106	33.00	−139.00	50–2000[a]	12[b]	60	–	18.9 (5.8)	799.7 (874.0)	42.6	12832	47.3	−0.521 (0.338)
107	34.23	−120.03	540	12	31	0.045	14.3 (3.3)	481.2 (541.4)	46.1	7068	33.3	−0.338 (0.062)
108	49.00	−174.00	4812	12	9	0.063	6.3 (6.9)	360.3 (564.0)	30.5	11832	39.5	0.325 (0.387)
109	49.00	−174.00	4812	12	12	0.063	6.3 (6.9)	360.3 (564.0)	31.3	6671	42.0	0.235 (0.459)
110	49.00	−174.00	4812	12	13	0.063	6.3 (6.9)	360.3 (564.0)	29.8	5681	36.9	0.021 (0.945)
111	49.00	−174.00	4812	12	10	0.063	6.3 (6.9)	360.3 (564.0)	29.0	4362	30.3	0.242 (0.497)
112	49.00	−174.00	4812	12	12	0.063	6.3 (6.9)	360.3 (564.0)	29.6	4639	28.4	−0.372 (0.229)
113	49.00	−174.00	4812	12	13	0.063	6.3 (6.9)	360.3 (564.0)	29.5	9173	30.1	0.085 (0.781)
114	49.00	−174.00	4812	12	13	0.063	6.3 (6.9)	360.3 (564.0)	29.9	6051	40.5	0.516 (0.067)
115	49.00	−174.00	4812	12	11	0.063	6.3 (6.9)	360.3 (564.0)	30.1	6563	41.0	0.549 (0.075)
116	49.00	−174.00	4812	12	14	0.063	6.3 (6.9)	360.3 (564.0)	31.9	3055	30.7	0.147 (0.616)
117	49.00	−174.00	4812	12	13	0.063	6.3 (6.9)	360.3 (564.0)	32.1	8221	35.3	0.318 (0.286)
118	50.00	−145.00	3800	12	23	0.063	8.1 (7.3)	395.5 (639.2)	31.4	36106	34.0	0.312 (0.146)
119	50.00	−145.00	3800	12	24	0.063	8.1 (7.3)	395.5 (639.2)	30.6	18958	34.9	0.174 (0.416)
120	53.32	149.83	258	12	21	0.063	3.7 (12.4)	438.0 (762.6)	22.4	192	19.4	0.288 (0.204)
121	53.32	149.83	1061	11	17	0.063	3.7 (12.4)	438.0 (762.6)	20.5	1013	29.3	0.563 (0.017)
122	53.50	−177.00	3198	12	13	0.063	5.2 (5.9)	408.1 (872.8)	29.1	10300	32.5	0.048 (0.876)
123	53.50	−177.00	3198	12	13	0.063	5.2 (5.9)	408.1 (872.8)	28.1	6972	34.6	0.376 (0.201)
124	53.50	−177.00	3198	12	10	0.063	5.2 (5.9)	408.1 (872.8)	25.7	3863	37.2	−0.280 (0.428)
125	53.50	−177.00	3198	12	11	0.063	5.2 (5.9)	408.1 (872.8)	25.7	4013	42.6	0.509 (0.104)
126	53.50	−177.00	3198	12	13	0.063	5.2 (5.9)	408.1 (872.8)	25.4	4004	30.3	−0.123 (0.688)
127	53.50	−177.00	3198	12	13	0.063	5.2 (5.9)	408.1 (872.8)	25.1	10636	39.2	−0.636 (0.017)
128	53.50	−177.00	3198	12	13	0.063	5.2 (5.9)	408.1 (872.8)	25.1	6301	41.3	−0.095 (0.757)
129	53.50	−177.00	3198	12	13	0.063	5.2 (5.9)	408.1 (872.8)	25.1	6930	37.2	−0.458 (0.111)
130	53.50	−177.00	3198	12	12	0.063	5.2 (5.9)	408.7 (872.8)	24.0	5961	38.7	−0.406 (0.185)
131	75.00	−162.00	184	12	26	0.045	−1.4 (0.9)	351.0 (603.5)	7.2	3475	19.2	0.333 (0.095)
132	75.00	−162.00	260	12	26	0.045	−1.4 (0.9)	351.0 (603.5)	6.6	2111	14.8	0.262 (0.195)
133	75.00	−162.00	1300	12	26	0.045	−1.4 (0.9)	351.0 (603.5)	7.2	6658	21.4	−0.071 (0.729)

[a]Mean for 12 depth intervals between 50 and 2000 m; [b]Discontinuous trapping intervals

While it can be argued that seasonal changes in species compositions are better reflected by taxonomic rearrangements between consecutive periods (rather than by the mean similarity between all possible sample pairs), mean RSCS based on consecutive samples only (i.e. sample 1 vs. sample 2, sample 2 vs. sample 3, etc.) were practically identical to the values based on all sample pairs within each series (correlation for all sample-to-sample similarities vs. similarities for consecutive samples only, Pearson's $R = 0.951$, $p < 0.001$, $N = 40$, Dataset 1). Low mean similarity values and high variability within each series are interpreted as indicative of strong seasonal changes in radiolarian assemblage compositions, whereas homogeneously high similarities suggest low seasonal differences in assemblage compositions.

Parametric statistics were used when raw or transformed data met the assumptions required (in particular, kurtosis and homoscedasticity). When test assumptions were not met, the statistical indicators were based on ranked values (non-parametric). For assessing the combined effects of the different variables on radiolarian flux, RFS, and RSCS, multivariate regression and multimodel selection were used (for details see 'Results: Multivariate analyses'). All analyses were performed with the aid of the pro-

Author copy

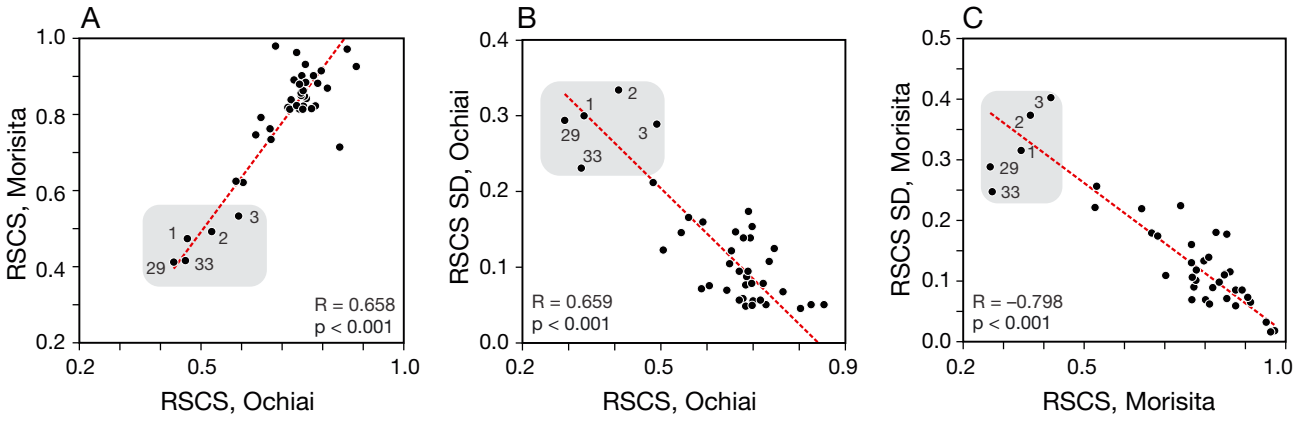


Fig. 2. (A) Concordance of mean sample-to-sample similarities as indicated by the binary Ochiai index and the quantitative Morisita index. (B,C) Relationship between mean and standard deviation (SD) of all sample-to-sample indices for the 40 sediment trap series with detailed taxonomic information (Dataset 1). RSCS: radiolarian specific composition stability. Lines are regressions for the raw values shown, R and p-values are based on Spearman's rank correlations. Labeled symbols (shaded area) denote series with lowest sample-to-sample similarity and highest variability

grams PAST (PAleontological STatistics, Ver. 2.17 and 3.14; Hammer et al. 2001), and SAM (Spatial Analysis in Macroecology, Ver. 4.0; Rangel et al. 2010).

RESULTS

Radiolarian flux rates and their intermittency

Radiolarian flux rates varied greatly between sites, spanning over 3 orders of magnitude (Fig. 3). Highest values were generally recorded at the low latitudes (~0 to 20° N), with several annual averages >20000 individuals (ind.) m^{-2} d^{-1}. High-latitude northern hemisphere sites yielded variable flux rates, including a few high values (e.g. series 36, 118), but mostly moderate to low ones (Tables 1 & 2, Fig. 3). The 3 sites from the Southern Ocean (series 1 to 3) were characterized by very low annual means. It should be noted, however, that while comparisons of temporal flux variability between series are robust, some absolute flux values are most probably affected by methodological differences (asterisked columns in Fig. 3; see 'Discussion').

Scatterplots of radiolarian flux rates and the environmental variables investigated are shown in Fig. 4, and the corresponding correlation values (including series where samples were sieved with ≥0.040 mm meshes only) in Table 3. Three series clearly stood out as outliers: 25, 36 and 118 (labeled in Fig. 4). Series 25, with the highest flux rates (Fig. 3), was based on unsieved materials (Boltovskoy et al. 1996). Series 36 and 118 are located in northern hemisphere high latitudes (~50 to 70° N), generally characterized by lower flux rates. Flux rate values as a function of the variables considered were generally dispersed (Fig. 4), but statistically significant ($p < 0.05$) in all cases, although the associations were often low (Table 3). Highest positive associations were with mean annual SST and PP half-time, whereas the strongest negative associations were with absolute latitude and ΔPP. RFS was highly correlated only with trap depth, and less markedly with ΔSST and radiolarian flux (Table 3).

Within-series temporal coupling between radiolarian flux rates and primary production (monthly means for 1997 to 2012, see 'Material and methods') was generally weak and showed little consistency. Of the 73 series analyzed, only 17 yielded positive and significant values (Spearman's R = 0.846 to 0.441, $p < 0.05$). Twenty series yielded negative correlation values (mean Spearman's R = –0.274), but only 1 of these was significant. On the other hand, these correlations (i.e. primary production vs. radiolarian flux rates) appear to be generally associated with mean annual PP, whereby at sites with low annual production (below ~300 gC m^{-2} yr^{-1}), seasonal changes in radiolarian flux match the timing of phytoplankton growth better than in areas of high PP (Fig. 5).

Radiolarian flux rates were positively associated with SST (and negatively with absolute latitude, which largely determines SST), PP half-time (and negatively with ΔPP, which in turn is associated with PP half-time), RFS, and trap depth (Table 3). Because flux rates are influenced by a combination of factors (see 'Multivariate analyses'), these pairwise contrasts offer useful hints on the underlying relationships, but

Author copy

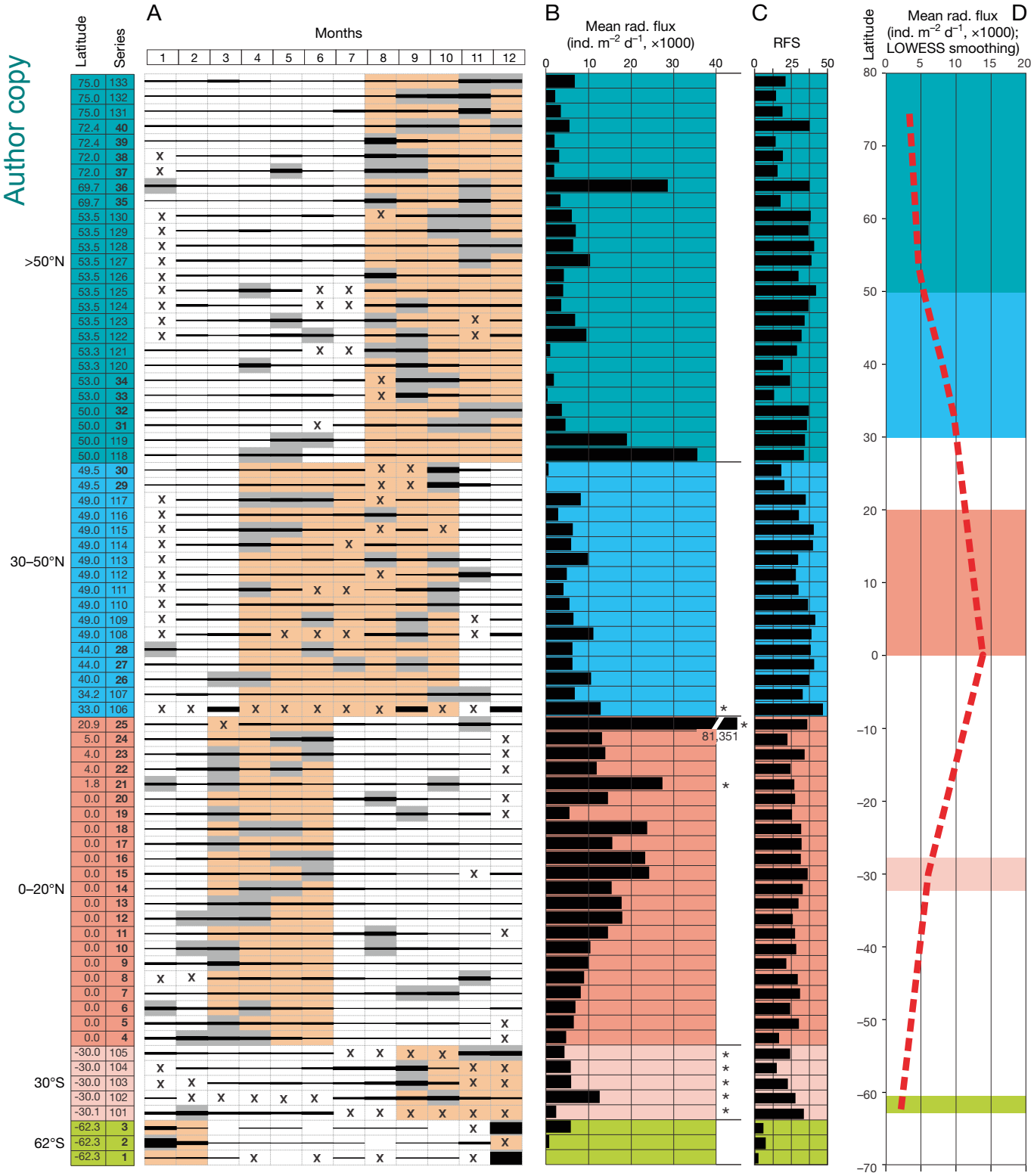


Fig. 3. Comparative values for radiolarian flux rates at all the sites surveyed, sorted in descending latitude (latitude offsets are highlighted with different colors). Bold numbers are from Dataset 1, non-bold are Dataset 2. (A) Monthly variations in radiolarian flux based on the mid-date of each collection period. Width of spindles is proportional to relative flux rates within each series, X symbols denote missing values (i.e. none of the midpoints of the trapping periods fell in the corresponding month). Grey cells denote values above mean +1 SD for each series. Orange shading denotes suggested periods of maximum flux for each latitudinal offset. (B) Mean flux for each series (see Tables 1 & 2 for details), missing values are not included in the averages; *counts performed on unsieved materials or samples sieved with ≤0.040 mm meshes. (C) Radiolarian flux stability (RFS). (D) Mean flux rates as a function of latitude (depth- and time-pooled data) based on a LOWESS smoothing function (Hammer et al. 2001; smoothing factor = 0.7), calculated for the northern and the southern hemispheres separately (merged in the graph); samples at 0° are included in both hemispheres, Series 25 is excluded from this estimate. Note that the vertical scale for (D) is not coincident with those for (A) to (C)

Author copy

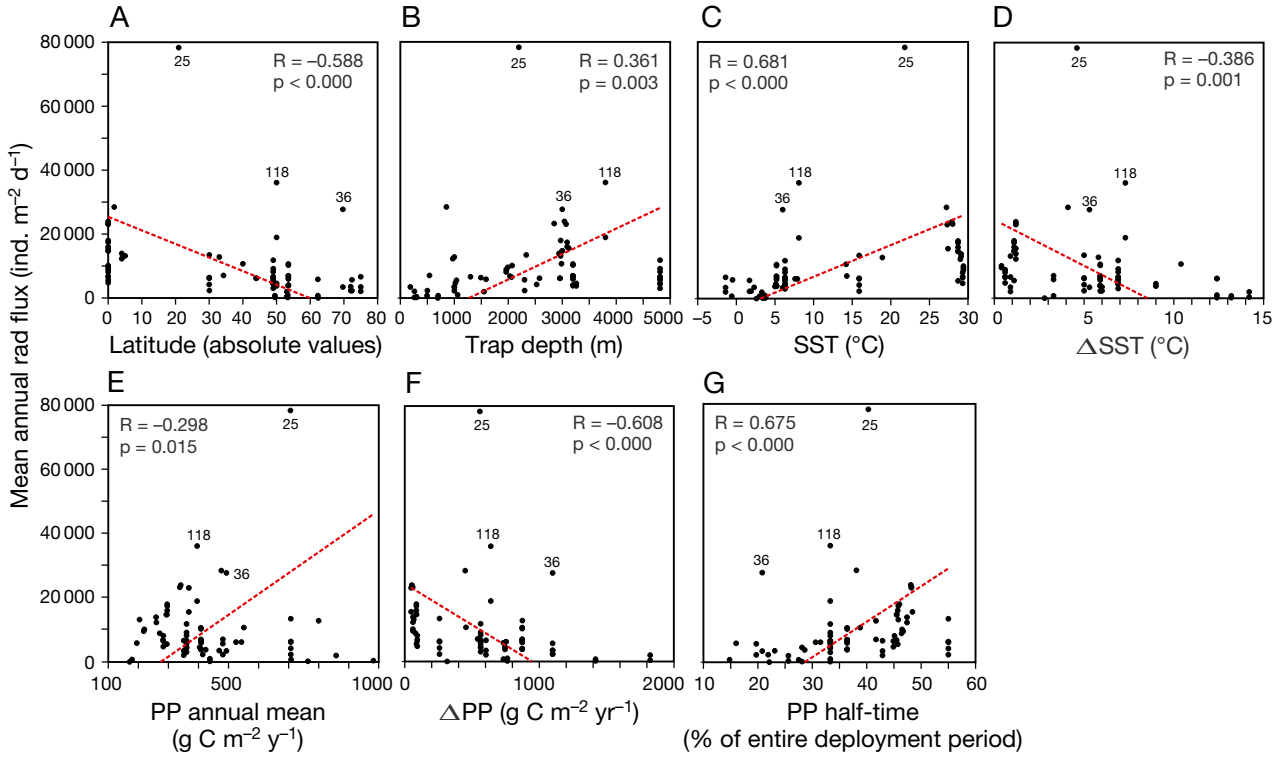


Fig. 4. Mean radiolarian (rad) flux rates versus environmental variables showing the 73 series analyzed. (A) latitude; (B) trap depth; (C) sea surface temperature (SST); (D) ΔSST; (E) annual mean primary production (PP); (F) ΔPP; and (G) PP half-time. Regression lines are based on all data, R and p-values are based on Spearman's rank correlations including the series which used samples sieved with 0.040 to 0.063 mm meshes only (Datasets 1 and 2; N = 66). In some cases, non-linear functions yielded slightly better fits than the linear ones shown, but the improvements were minor and did not switch the significance levels from $p < 0.05$ to $p > 0.05$, or vice versa). Labeled series denote outliers

conceal the strength of some. Trap depth, in particular, seems to have a much more important effect on flux rates than suggested by the corresponding significant, albeit rather low, correlation value (Spearman's R = 0.361, Table 3). Comparison of simultaneous deployments at 2 different depths 400 to 2000 m apart show that the lower trap invariably yielded higher fluxes (Fig. 6A) and higher RFS values (10 of 11 comparisons, Fig. 6B) than the upper one. In terms of timing, radiolarian fluxes in the upper trap of each pair were generally uncoupled from the fluxes recorded by the lower trap: only 4 pairs (22–23,

Table 3. Pairwise Spearman's correlations and p-values between radiolarian (rad.) flux rates and radiolarian flux stability (RFS) and environmental variables. Series included are those which used samples sieved with 0.040 to 0.063 mm meshes only (Datasets 1 and 2; N = 66). **Bold** values denote statistically significant values ($p < 0.05$). Abs. lat.: absolute latitude; PP: primary production; SST: sea surface temperature. See Tables 1 & 2 for sources and units

	Mean rad. flux		RFS	
	R	p	R	p
Abs. lat.	**−0.588**	**0.000**	−0.122	0.329
Trap depth	**0.361**	**0.003**	**0.733**	**0.000**
SST annual mean	**0.681**	**0.000**	0.183	0.142
ΔSST	**−0.386**	**0.001**	**0.286**	**0.020**
PP annual mean	**−0.298**	**0.015**	0.241	0.051
ΔPP	**−0.608**	**0.000**	0.006	0.961
PP half-time	**0.675**	**0.000**	0.195	0.117
Mean rad. flux			**0.386**	**0.001**
RFS	**0.386**	**0.001**		

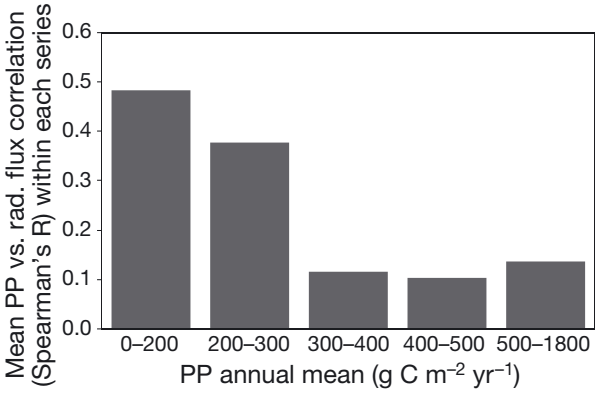


Fig. 5. Coupling between the seasonal changes in primary production (PP) and radiolarian (rad.) flux rates as a function of the mean annual primary production at the sediment trap sites investigated

Author copy

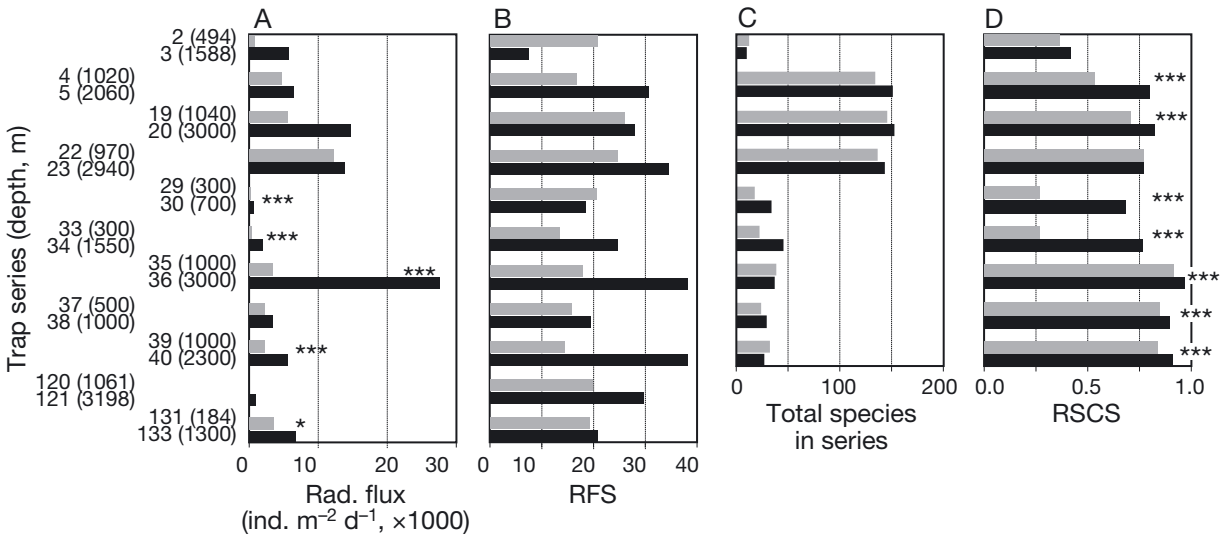


Fig. 6. Comparison of (A) radiolarian (Rad.) flux, (B) radiolarian flux stability (RFS), (C) total species recorded, and (D) radiolarian specific composition stability (RSCS) for simultaneous or quasi-simultaneous series of sediment trap samples deployed at different depths at the same site. Statistically significant differences between the 2 depths compared are denoted with asterisks (*$p < 0.05$, ***$p < 0.001$; Kruskal-Wallis)

29–30, 37–38, and 120–121) yielded statistically significant correlations ($p < 0.05$, Spearman's R) between the flux in both traps, and in 3 cases the correlations were negative (albeit none of them significant). Shifting the values of the lower trap 1 or 2 positions forwards (~15 to 60 d; in order to account for the time delay in the flux peaks reaching the lower trap) did not improve these values.

The association between mean radiolarian flux rates and their corresponding RFS values based on all the series which used ≥0.040 mm sieves (where radiolarian counts were presumably unbiased by methodological artifacts; see 'Material and methods' and 'Discussion') were positive and significant but low (Table 3). RFS was strongly associated with trap depth, and marginally with ΔSST (Table 3).

Variations in radiolarian species compositions

For these analyses, only Dataset 1 (which included detailed information on all the species recorded in each sample, Table 1) was used. Within most of the series, the numbers of species recorded in each sample were positively associated with the corresponding radiolarian flux values ($p < 0.05$ for 29 of the 40 series analyzed, Spearman's R). However, these values were clearly affected by differences in the numbers of radiolarian specimens counted in each sample. Of the 27 series where the original sources provided information on the numbers of specimens per sample identified, 25 showed positive and significant (Spearman's R = 0.461 to 0.981, $p < 0.05$) associations between specimens identified and number of species recorded ($p < 0.01$ for 22 series). Individual rarefaction (which allows estimating species richness values in samples of different sample size; Hammer et al. 2001) applied to the series with highest correlations between specimens identified and species recorded (Spearman's $R > 0.9$, series 4, 5, 20, 23, 24, 33), and restricted to samples with >50 specimens, indicated that rarefacted species richness values were not correlated with radiolarian flux. Thus, the temporal association between absolute radiolarian flux and species richness suggested by some surveys (e.g. Lange et al. 1997) could not be confirmed in the present study. A similar problem was also encountered when attempting to assess the relationship between mean radiolarian flux rates and mean species richness geographically. The association was significant (Spearman's R = 0.623, $p < 0.001$; Table 4), but for 25 (of the 27 series with data on individuals counted), mean numbers of species were significantly associated with mean numbers of specimens identified in each series (Spearman's R = 0.797, $p < 0.001$).

RSCS values were generally high, with the exception of 3 series in the Southern Ocean (1 to 3), and 2 shallow (300 m) trap series in the Sea of Okhotsk (29 and 33; Figs. 1, 2 & 3) (see 'Discussion'). Variations in sample-to-sample similarity (RSCS SD) were clearly less marked when similarity values were homogeneously high (rather than homogeneously low), as indicated by the very significant negative association between RSCS and RSCS SD (Table 4, Fig. 2B,C).

Author copy

Table 4. Pairwise linear correlation values (Spearman's R) between environmental variables and flux values with faunal data. All indices are based on 40 series (Dataset 1), except for those with mean radiolarian (rad.) flux, which are based on the 38 series which used ≥0.040 mm sieves. **Bold** values: p < 0.01; Abs. lat.: absolute latitude; PP: primary production; RFS: radiolarian flux stability; RSCS: radiolarian specific composition stability; SST: sea surface temperature

	Total species in series		RSCS		RSCS SD	
	R	p	R	p	R	p
Abs. lat.	**−0.699**	**0.000**	0.025	0.876	0.045	0.784
Trap depth	0.371	0.018	**0.451**	**0.003**	−0.340	0.032
SST annual mean	**0.806**	**0.000**	−0.068	0.678	−0.081	0.620
ΔSST	**−0.639**	**0.000**	0.042	0.796	0.018	0.911
PP annual mean	−0.330	0.037	0.299	0.061	−0.263	0.101
ΔPP	**−0.691**	**0.000**	−0.077	0.636	0.093	0.567
PP half-time	**0.750**	**0.000**	0.074	0.649	−0.133	0.412
Mean rad. flux	**0.623**	**0.000**	**0.435**	**0.006**	−0.386	0.017
RFS	0.336	0.034	**0.461**	**0.003**	**−0.486**	**0.001**
Total species in series			0.192	0.235	−0.288	0.072
RSCS	0.192	0.235			**−0.798**	**0.000**
RSCS SD	−0.288	0.072	**−0.798**	**0.000**		

Mean sample-to-sample similarities (RSCS) were positively associated with trap depth (Table 4, Fig. 7C), but this association was clearly driven by the 5 'anomalous' series (labeled in Fig. 7C): exclusion of these 5 data points yielded a non-significant correlation (Spearman's R = 0.197, p = 0.256). Nevertheless, comparison of 18 simultaneous series at different depths showed that the lower trap of each pair usually yielded higher numbers of species (6 of 9 comparisons; Fig. 6C), and always higher RSCS values (statistically significant in 7 cases; Fig. 6D).

RSCS was strongly associated with radiolarian flux, the relationship being best described by a logarithmic function, with RSCS values tending to stabilize around 0.8 to 0.9 above yearly mean values of approximately 15000 ind. m^{-2} d^{-1} (Fig. 7B).

As expected, the total numbers of species recorded in each series were closely coupled with latitude (and with SST, ΔSST, ΔPP, and PP half-time, all associated with latitude; Table 4), with highest values in the tropics and subtropics, decreasing gradually towards the higher latitudes of both hemispheres (see Boltovskoy & Correa 2017). The mean flux values and the total number of species recorded in each of the 40 series (Dataset 1, pooled samples), as well as mean specific diversity (as measured by the Shannon-Wiener index) were highly correlated (Spearman's R = 0.753 for number of species, R = 0.610 for specific diversity, p < 0.001 in both cases). However, as noted above, these associations were influenced by dissimilar sample sizes.

Multivariate analyses

As in the previous section, these analyses were based on Dataset 1 only (Table 1), which included detailed specific makeup information. Analysis of the combined effects of different variables on radiolarian flux, RFS, and RSCS was hampered by the fact that many of the values detailed in Table 1 are intercorrelated (p < 0.05 for 74% of the pairwise correlations), restricting the combined use of the inde-

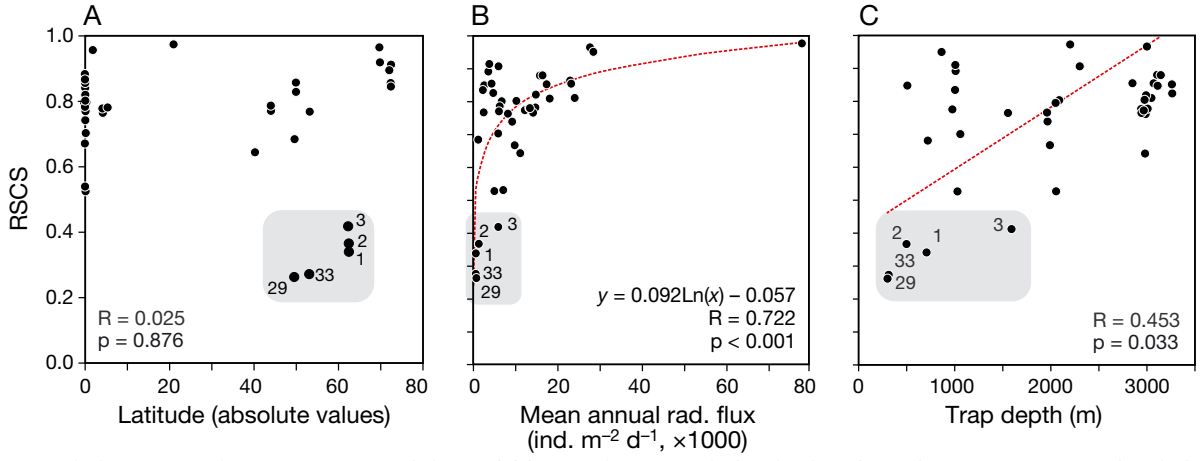


Fig. 7. Radiolarian specific composition stability (RSCS) as a function of (A) absolute latitude, (B) mean annual radiolarian (rad.) flux, and (C) trap depth for 40 series of sediment traps (Dataset 1). Labeled symbols (shaded area) denote series with lowest sample-to-sample similarity. Regression lines are based on Ln-transformed (B; Pearson's R and p-values) or raw data (C; Spearman's R and p-values)

Author copy

Table 5. Linear multiple regressions between the variables analyzed based on mean values for each sediment trap series. Only variables whose variance inflation factor (VIF) values were <5 are included, all other environmental traits yielded VIF > 10, and their inclusion did not increase the overall R^2 markedly. PP: primary production; Rad. flux: radiolarian flux

Independent variables	Coeff.	SE	*t*	R^2	p	VIF
Dependent variable: Mean annual radiolarian flux (R^2 adj. = 0.616; *F* = 15.928; p < 0.001)						
Constant	17.644	6.430	2.744		0.010	
Trap depth (m)	0.281	0.121	2.323	**0.380**	0.026	1.129
SST (°C)	0.136	0.146	0.927	0.281	0.360	1.506
PP (gC m^{-2} yr^{-1})	0.358	0.142	2.513	0.022	0.017	1.370
ΔPP (gC m^{-2} yr^{-1})	−0.658	0.183	−3.594	**0.447**	0.001	3.483
Dependent variable: RFS (R^2 adj. = 0.654; *F* = 15.115; p < 0.001)						
Constant	−7.779	6.728	−1.156		0.256	
Trap depth (m)	0.618	0.123	5.005	**0.570**	0.000	1.691
SST (°C)	0.159	0.141	1.132	0.054	0.266	2.163
PP (gC m^{-2} $yr^{-1)}$	0.325	0.147	2.217	0.068	0.033	2.369
ΔPP (gC m^{-2} yr^{-1})	0.082	0.203	0.404	0.056	0.688	4.769
Rad. flux	0.208	0.160	1.295	0.326	0.204	2.820
Dependent variable: RSCS (R^2 adj. = 0.429; *F* = 5.555; p < 0.001)						
Constant	−1.024	8.815	−0.116		0.908	
Trap depth (m)	0.244	0.209	1.169	0.212	0.251	2.936
SST (°C)	−0.250	0.184	−1.357	0.004	0.184	2.244
PP (gC m^{-2} yr^{-1})	0.113	0.202	0.561	0.089	0.578	2.711
ΔPP (gC m^{-2} yr^{-1})	0.273	0.262	1.043	0.002	0.304	4.792
Rad. flux	0.722	0.211	3.420	**0.265**	0.002	2.959
RFS	−0.040	0.220	−0.179	0.216	0.859	3.223

pendent variables involved due to potential multicollinearity-related biases (Belsley et al. 1980). Thus, a stepwise model selection procedure was used (Rangel et al. 2010), whereby different numbers of independent variables are incorporated and the resulting Akaike's information criteria and variance inflation factors allow selection of the best model and minimize the effects of collinearity. Because the response variables are nested (radiolarian flux depends on environmental traits, RFS is dependent on the latter and on radiolarian flux, and RSCS is dependent on all of the above), variables were incorporated in a stepwise manner (Table 5). In all 3 assessments, multiple adjusted R^2 values were moderate but highly significant. Partial R^2 were mostly low, but generally confirmed the most salient relationships observed in the pairwise comparisons shown in Tables 3 & 4.

DISCUSSION

Limitations and caveats

Before interpreting the results of the analyses performed, some important considerations must be kept in mind.

The production (or flux) half-time concept has been used repeatedly in studies and has yielded consistent results (Berger & Wefer 1990, Lampitt & Antia 1997, Brown et al. 2014), but it does have shortcomings. The assumption that low half-production times reflect highly punctuated production modes where most of the matter is delivered in a short period of time, whereas high values indicate a more even production profile relies on the premise that the peaks in spiked profiles (i.e. low half-production times) are centered on 1 or a few periods of the year, whereas less variable modes, characterized by a more even profile, result in high half-production times. When months are used as the base unit for the estimates, the 2 extreme situations are (1) when the entire annual production occurs in a single month (half-production time: 1 mo; Fig. 8A,B) and (2) when all 12 months have identical production values (half-production time: 6 mo; Fig. 8G). In both these cases, the index adequately reflects the production mode. On the other hand, intermediate index values can be due to at least 4 quite dissimilar situations: (1) seasonal cycles with peak production in the middle of the trapping period and evenly decreasing values towards both extremes (Fig. 8C); (2) cycles with all the yearly production evenly distributed throughout 6 consecutive months of the year (Fig. 8D); (3) an intermittent production

Author copy

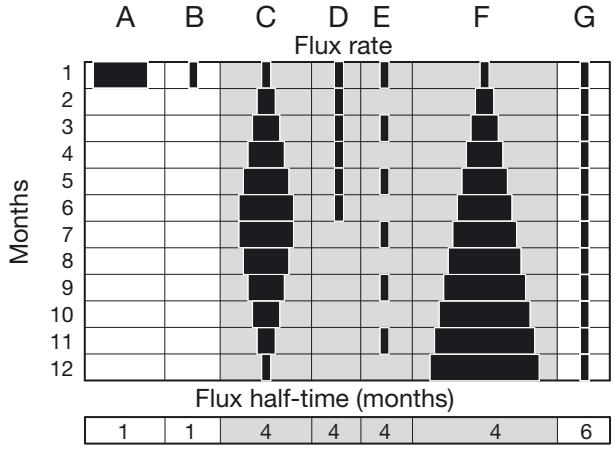


Fig. 8. Conceptual representation of flux (or productivity) values throughout a 12 mo period and the resulting figures of flux (or productivity) half-time (mo). Panels A to G represent different modes of flux production during the year. Note that quite dissimilar flux profiles can yield identical flux half-times (grey columns)

mode of successive months with equal production and without production (Fig. 8E); and (4) profiles with evenly increasing (or decreasing) values from start to end (Fig. 8F). All these situations yield an identical half-production time value of 4 (Fig. 8C–F). Thus, while the significance of extreme half-production index values (1 or 6) does not lend itself to misinterpretation, the cycles that yield intermediate values are more difficult to ascertain from the index alone. These cycles might not represent a major problem when the temporal distribution of production peaks is marginally relevant to the problem investigated like, for example, the association between primary production cycles and export production (Berger & Wefer 1990, Lampitt & Antia 1997). On the other hand, when production (or flux) cycles are investigated in terms of their coupling with assemblage-specific compositions (as in this work), these different situations leading to identical half-production time indices may obscure interpretations. In practice, however, such extreme situations as the profiles illustrated in the grey columns of Fig. 8 are apparently not common (Fig. 3). Further, to investigate the effect of sorting flux values from highest to lowest on the RFS indices, they were recalculated on a monthly basis without sorting, but ordered chronologically starting with the highest flux value in the first month (Dataset 1). The resulting indices closely followed the RFS values used (Pearson's $R = 0.854$, $p < 0.001$). As expected, the match was perfect up to half-flux times of 3 mo, whereas the mismatches were more pronounced at higher values.

Another potential concern is that the numbers of radiolarians counted per sample varied widely, from a mean of 5.3 to 297 individuals per series (for the 27 series for which information was supplied in the original reports, Dataset 1), and a few samples (5 out of a total of 823) yielded no radiolarians at all, and they were therefore incorporated in RFS calculations (as zeros), but not in the RSCS estimates. While there are no reasons to assume that radiolarian flux values and RFS were homogeneously under- or overestimated by these differences in numbers of individuals counted, these dissimilarities might have had an effect on RSCS values in the series with lowest specimen counts. Indeed, lowest RSCS figures were found for the series with <30 radiolarians per sample identified (series 1 to 3, 29 and 33, Dataset 1), and these series were singled out in most of the analyses performed (Figs. 2 & 7), and excluded from some estimates (Table 4, Fig. 9H). Nevertheless, these suspect data points do not seem to affect the overall trends described. For series with a mean of >40 specimens per sample identified (sample size), the correlation between mean sample size and mean RSCS was very low and statistically non-significant (Spearman's $R = 0.228$, $p = 0.308$, $N = 22$). Further, the latitudinal gradients suggested are also supported by the fact that mean sample size was uncorrelated with latitude (absolute latitude vs. sample size, Pearson's $R = -0.275$, $p = 0.166$, $N = 27$; log-transformed data).

Comparison of radiolarian fluxes between series is also hindered by the fact that most surveys (66 series, 92% of the samples) counted the radiolarians retained by 0.040 to 0.063 mm mesh sieves, but 1 series used a smaller mesh (0.015 mm, series 21), and 6 series did not sieve the samples at all (Tables 1 & 2). Sieve size has been observed to affect radiolarian abundance estimates significantly (Beers & Stewart 1971, Caron & Swanberg 1990, Boltovskoy & Alder 1992a,b, Boltovskoy 2017). While averaged flux rates for all the samples as a function of sieve size yielded a low and statistically non-significant correlation (Spearman's $R = 0.142$, $p = 0.230$), flux values binned in the 5 mesh-size classes used (unsieved, 0.015, 0.04, 0.045, and 0.063 mm) showed significant differences between the yields of meshes ≤0.015 mm and meshes ≥0.040 mm (Kruskal-Wallis test and Mann-Whitney Bonferroni-corrected contrasts). These differences suggest that approximately 8% of the absolute flux values used in this review are marginally comparable with the bulk of the data, a source of bias that, as explained above, was taken into account in the estimates performed.

Author copy

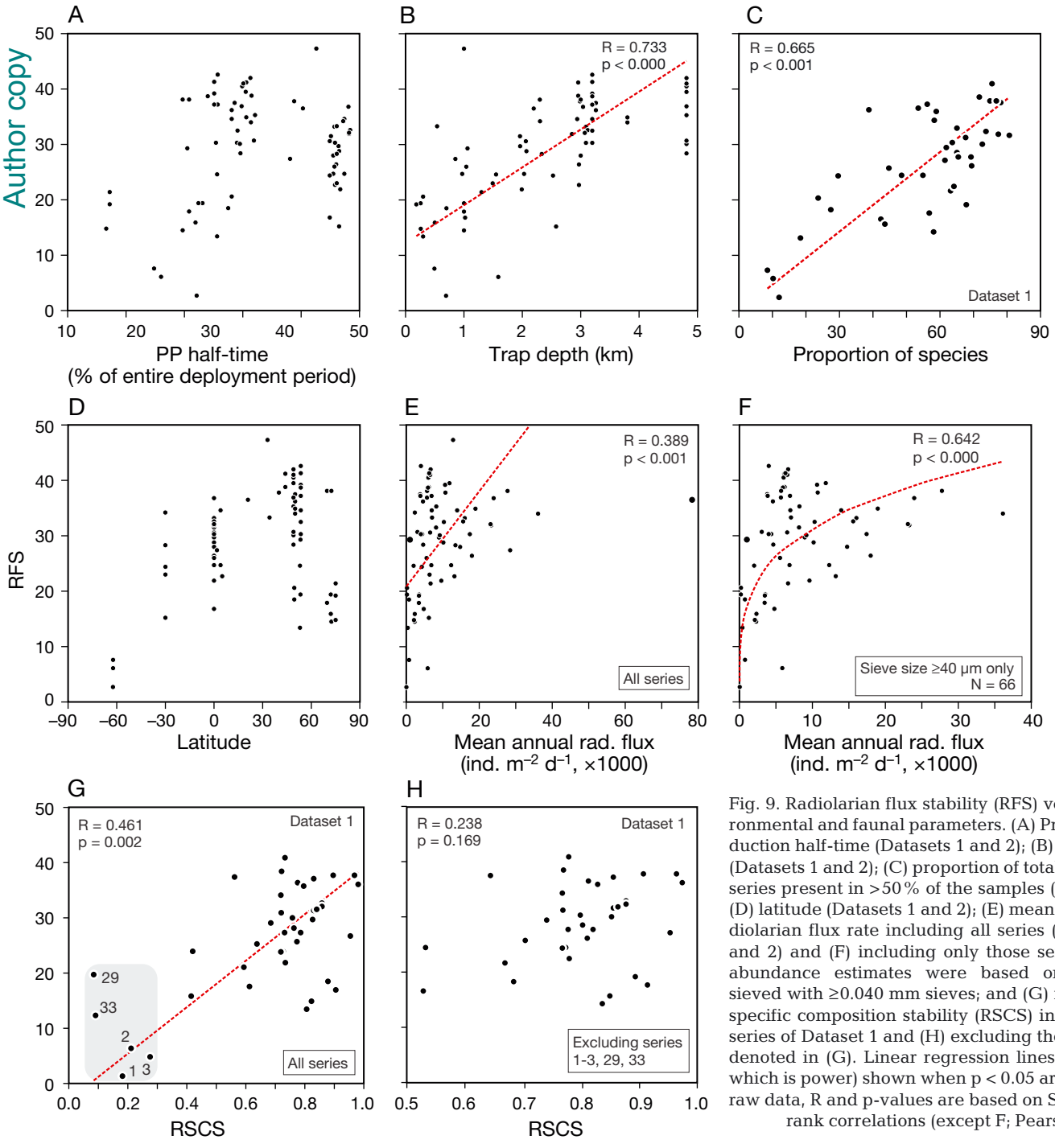


Fig. 9. Radiolarian flux stability (RFS) versus environmental and faunal parameters. (A) Primary production half-time (Datasets 1 and 2); (B) trap depth (Datasets 1 and 2); (C) proportion of total species in series present in >50% of the samples (Dataset 1); (D) latitude (Datasets 1 and 2); (E) mean annual radiolarian flux rate including all series (Datasets 1 and 2) and (F) including only those series where abundance estimates were based on samples sieved with ≥0.040 mm sieves; and (G) radiolarian specific composition stability (RSCS) including all series of Dataset 1 and (H) excluding the 5 outliers denoted in (G). Linear regression lines (except F, which is power) shown when $p < 0.05$ are based on raw data, R and p-values are based on Spearman's rank correlations (except F; Pearson)

On the other hand, relative variations in flux values, and therefore comparisons of RFS figures between series, are probably not affected by this bias. In the surveys that used unsieved samples (Boltovskoy et al. 1996, series 25), or samples sieved with a 0.015 mm screen (Boltovskoy et al. 1993, series 21), associations between total radiolarian flux and the flux of the smaller forms (which were conceivably missed in studies that employed larger-pore sieves; chiefly members of the family Plagoniidae and juvenile, mostly unidentified, radiolarians) were very high (Spearman's R = 0.912 and 0.993, respectively; $p < 0.001$), suggesting that the fraction of the radiolarians under-represented in the materials which used 0.040 to 0.063 mm sieves is roughly similar across samples and surveys. Thus, while the absolute flux values for some of the series covered have some caveats and are conceivably marginally comparable

Author copy

with the rest (for which reason they are treated separately in the analyses performed), contrasts in the temporal variability of the flux rates and species compositions are likely unaffected by these methodological differences.

It should also be borne in mind that all our estimates are based on single 11 to 12 mo periods, and therefore interannual variations, which can be significant in some areas (Takahashi 1987, Lange et al. 1997, Ikenoue et al. 2012a), are accounted for only at those sites where more than 1 annual series was available. Further, while radiolarian data are based on samplings conducted during different time offsets between 1983 and 2003, SST and PP are mean values for 1955 to 2012 and 1997 to 2012, respectively, which may be only marginally representative of some of the radiolarian sampling periods. These mismatches, however, are unlikely to have strongly biased our analyses, because most of the sediment trap sites investigated are located in areas where SST and chlorophyll *a* concentrations display moderate interannual variations, as shown by data between 1998 and 2010 analyzed by Fay & McKinley (2014).

Lastly, it is important to note that there are many areas of the World Ocean that are under-represented in the employed database, or missing altogether. These areas include most of the Southern Ocean, the Indian Ocean, the South Atlantic, the eastern Pacific, and the western North Atlantic (Fig. 1). Adequate radiolarian flux data are unavailable for these regions. Further, while the tropics and the northern polar and subpolar waters are fairly well represented, only 3 series from the Southern Ocean were available, and the middle latitudes of both hemispheres are poorly represented (Fig. 1). This lack of information from subtropical and transitional areas is most probably responsible for the fact that some of the results show the trap sites clustered at the 2 extremes of what one would intuitively expect to be a gradient (e.g. Fig. 9G).

These limitations restrict the conclusions arrived at in this report, which should therefore be regarded as preliminary.

Radiolarian flux rates and flux stability

Judging from the information available, radiolarian flux rates are highest in the tropics and subtropics, generally decreasing towards the high latitudes, especially in the Southern Ocean (Figs. 3B,D, 4A, & 10). Locally, mean annual flux rates are strongly associated with trap depth, and geographically with

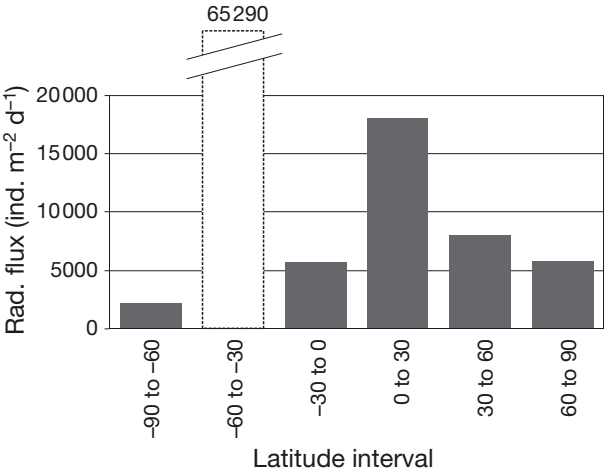


Fig. 10. Radiolarian (Rad.) flux rates based on depth- and time-averaged values for all sources listed in Tables 1 & 2. Data for 30 to 60° S (white bar) are based on a single work from a highly productive area off the coast of Chile (5 time-series deployments at 1492 to 2578 m, covering 180 to 260 d), which used unsieved materials and, therefore, are not likely to be comparable to most other data

SST, PP half-time, ΔPP, and absolute latitude, but, somewhat surprisingly, very weakly with PP mean annual values (Tables 3 & 5, Fig. 4).

Fig. 11 shows the sites investigated (Dataset 1) grouped into 3 categories according to their RFS values. The first group (Fig. 11A), which only includes the 3 sites from the Southern Ocean, is characterized by the lowest PP, radiolarian flux rates, and RFS. These trap sites were free of ice for only about 30% of the trapping time, the remaining 70% of the time being covered by sea ice, or in the area where the ice edge shifted back and forth (Abelmann 1992). Clearly, in this case, low radiolarian flux rates coincide with low PP, low PP half-times, and low RFS. However, series 29, 30, and 34, at approximately 50 to 53° N in the Sea of Okhotsk, which were also ice-covered for approximately 30% of the time (and radiolarian flux was ca. 3 times lower than during ice-free periods; Okazaki et al. 2003), associations with PP pulses were non-significant (series 29 and 34), or low (series 30; Table 1). In the western Arctic Ocean (75° N, 162° W), associations between radiolarian flux and sea-ice cover (when primary production is lowest), were also very low and non-significant (series 131 to 133 in Table 2, Ikenoue et al. 2015). Although RFS was low (~15 to 20), correlations between sea-ice cover (%) and flux at this site were negative but very low and statistically non-significant (Spearman's R = –0219, $p > 0.05$, N = 78, pooled data). Contrasts between the temporal stability of the vertical flux between high latitude northern and southern waters

Author copy

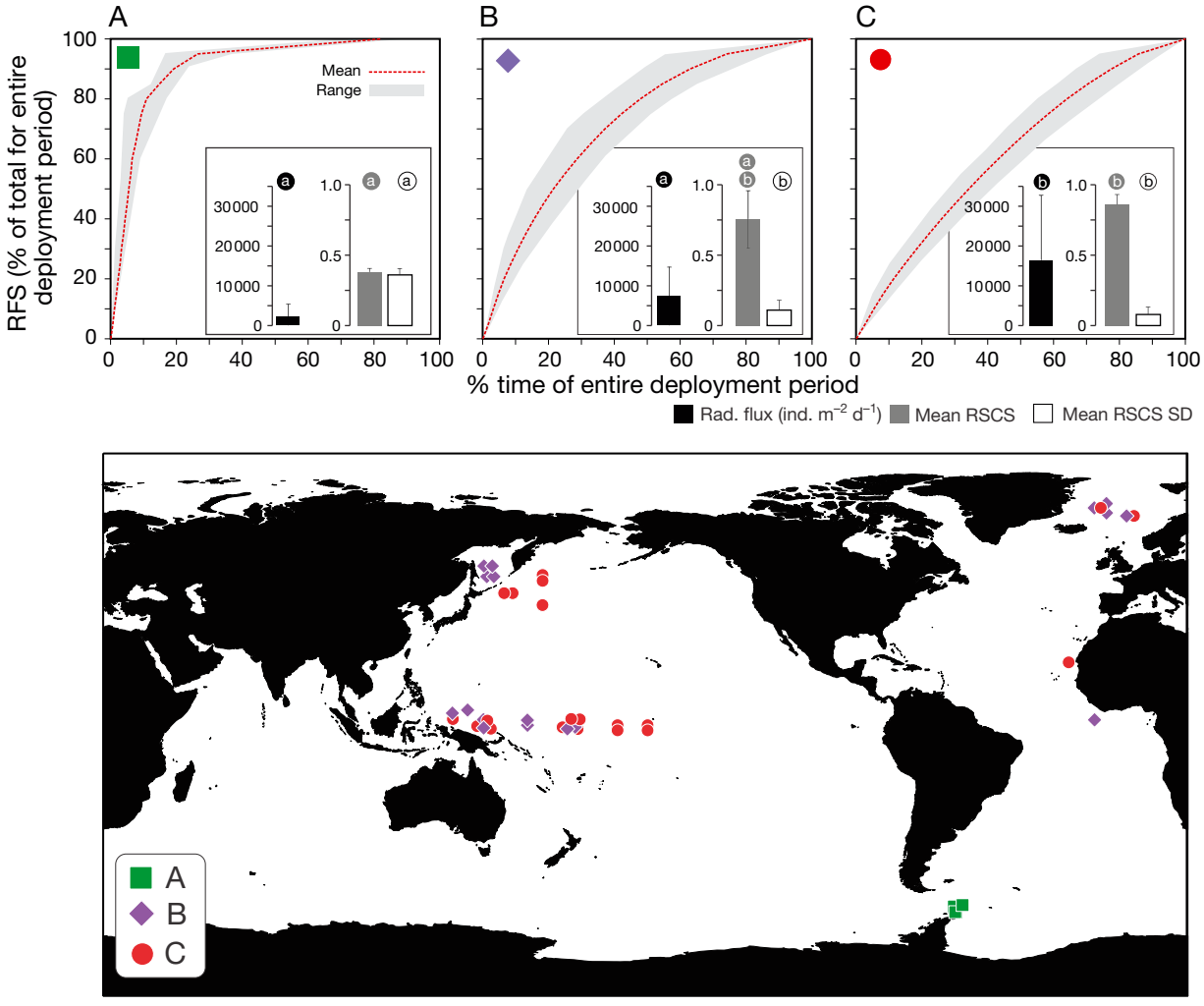


Fig. 11. Intermittency in radiolarian flux stability (RFS) for the series investigated (Dataset 1) grouped in 3 categories: (A) 50% of the total flux in 3 to 8% of the overall trap deployment time (Series 1 to 3); (B) 50% of the total flux in 13 to 29% of the overall trap deployment time (Series 4, 6, 9, 10, 12, 19, 21, 22, 24, 29, 30, 33 to 35, 37 to 39); and (C) 50% of the total flux in 28 to 41% of the overall trap deployment time (Series 5, 7, 8, 11, 13 to 18, 20, 23, 25 to 28, 31, 32, 36, 40). Groups were defined using Jenks' natural breaks. The 3 groups of values for 50% of total flux are significantly different at $p < 0.001$ (1-way ANOVA and Tukey's pairwise comparisons). Grey area envelopes all curves within each category; red dotted line denotes the mean value. Inset graphs show mean radiolarian (Rad.) flux, mean radiolarian specific composition similarity (RSCS), and mean SD of all within-series similarities (RSCS SD). Notice that error bars are SD between series (only positive values are shown), while white bars are mean SD of all within-series values. Different letters above bars denote significant differences at $p < 0.05$ (Kruskal-Wallis and pairwise Mann-Whitney contrasts). The geographic locations of the sediment trap series included in each group are shown underneath

have been noted before (Lampitt & Antia 1997), and are probably associated with the fact that the Southern Ocean is more efficient than the Arctic in recycling a large proportion of the organic production in the upper ocean (thus restricting downward flux, especially at times of low near-surface production; Smetacek et al. 1990). In addition, the limiting effects of nutrient availability in the Arctic (which can hinder production and flux when light availability and vertical stability are favorable; Lalande et al. 2014) and occurrence of phytoplankton blooms under Arctic sea ice (Arrigo et al. 2012) can also smooth out radiolarian growth and flux peaks. This weak association between PP pulses and pulses in radiolarian flux is illustrated in Fig. 12, where both intermittencies at the sites investigated are graphed as a function of absolute latitude. PP half-times are quite regularly aligned with highest values near the equator and lowest ones towards the poles, whereas RFS figures show no latitudinal pattern.

The second and third groups of sites shown in Fig. 11B,C (the RFS of which obviously differ very

Author copy

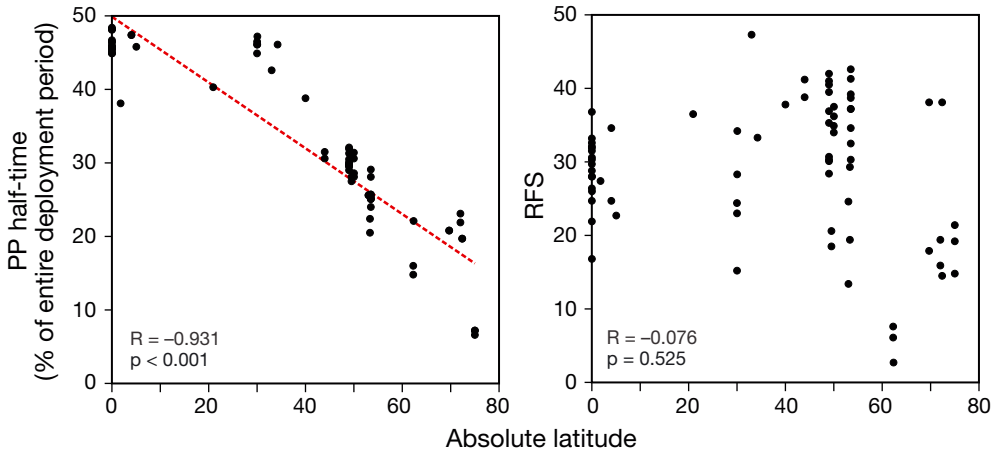


Fig. 12. Primary production (PP) half-time and radiolarian flux stability (RFS) as a function of latitude (absolute values; Datasets 1 and 2). Regression line is based on raw data, R and p-values are based on Spearman's rank correlations

significantly because this is the criterion used for separating them), have statistically undistinguishable radiolarian fluxes, and are widely dispersed geographically. In summary, our analyses suggest that, on the geographic scales used in this work, mean annual radiolarian fluxes are not coupled with mean annual PP. On the other hand, at each site, the seasonal association between PP and radiolarian flux is variable: in areas where PP is generally low (up to ca. 300 gC m^{-2} yr^{-1}), radiolarian fluxes tend to increase following the (often short, usually a few weeks to 1–3 mo) periods of enhanced productivity, but when mean PP is moderate or high, radiolarian fluxes are not associated with phytoplanktonic growth (Fig. 5).

In terms of the timing of flux peaks throughout the year, except for the 3 Southern Ocean sites where flux is practically restricted to the summer, maxima in flux rates vary greatly in the tropics–subtropics and in northern hemisphere cold waters (Fig. 3), and even in the Arctic, highest values often occur under ice-covered waters (Ikenoue et al. 2015).

Comparison of RFS in sediment trap samples with seasonal variations of radiolarian standing stocks in the water column is hindered by the fact that there are very few seasonal radiolarian plankton collections. Monthly data collected in a Norwegian fjord (60.18° N) from depths of 0 to 670 m (Bjørklund 1972, 1974) indicate that the RFS based on depth-averaged density (rather than flux) values for the offset 25 November 1969 to 24 November 1970 is 24.1. This RFS is generally within the range of values of northern hemisphere high latitude areas (Fig. 9D). A similar analysis for a plankton collection from the area of the California Current (6 January to 16 November 1972, forty-eight 0 to 100 m vertical tows at ~24 to 36°N, nominal month-pooled data; Boltovskoy & Riedel 1987) yielded an RFS value of 27.3, again not too different from the numbers for many sediment trap samples (Fig. 9D).

Local and regional investigations of the temporal and/or spatial coupling between radiolarian fluxes and measured or inferred PP have arrived at dissimilar conclusions, ranging from weak, inconclusive, or no association at all (Takahashi 1987, Gowing 1993, Lange et al. 1997, Motoyama et al. 2005, Okazaki et al. 2005, Venrick et al. 2006), to moderately or clearly defined flux pulses during or shortly after PP peaks near the surface (Abelmann 1992, Boltovskoy et al. 1993, 1996, Takahashi 1997, Hays & Morley 2003, Okazaki et al. 2008, Lampitt et al. 2009). It should be stressed that these results are based on all radiolarians, and do not take into account variations in the flux of individual species, some of which have been reported to correlate with PP cycles, whereas total radiolarians did not (see below).

Data on total mass flux and the flux of other shelled microplankton are mixed as well. For planktonic Foraminifera, for example, several surveys have reported more or less well defined associations between various proxies of PP and shell flux (Eguchi et al. 1999, King & Howard 2001, Asahi & Takahashi 2007), while others have found very marked differences between closely spaced trap sites with very similar seasonality (King & Howard 2003). Thus, while there is adequate consensus that the stability of PP and that of overall flux decrease with increasing latitude (Lampitt & Antia 1997, Brown et al. 2014, Anabalón et al. 2016), absolute levels of flux vary widely geographically (Lampitt & Antia 1997), and depend on multiple variables including, among others, the mineral ballast composition of sinking material, particle size, denitrification processes, and midwater biological activity (Takahashi 1987, Smetacek et al. 1990, Lima et al. 2014).

An important confounding factor in the coupling of radiolarian flux rates with PP may stem from the fact that these organisms overlap 2 ecological niches.

Author copy

Species which host symbiotic algae are less dependent on the availability of external food sources for survival, whereas species that do not have autotrophic symbionts are more likely to be able to thrive only when phytoplankton is abundant. Further complications may arise from seasonally changing oceanographic settings unassociated with PP, such as the shifts in the dominant currents or the input of low salinity waters due to ice melting or continental runoff (Suzuki & Not 2015). Continental runoff can also conceivably enhance radiolarian production through the input of dissolved silica, used by these protists to build their skeletons, although on worldwide scales, dissolved Si at 0 and 1500 m is not associated with radiolarian densities in the sediments (Boltovskoy et al. 2010, their Fig. 7.1).

The positive associations between radiolarian flux rates and depth observed in the data reviewed (Fig. 6A) are probably in part the result of environmental settings, but methodological factors seem to play a key role. In cold-water areas, higher flux rates at depth may reflect the fact that radiolarian standing stocks peak at approximately 200 to 400 m (Hays & Morley 2003, Boltovskoy 2017; note, however, that only 6 of the 73 sediment trap series used were deployed above 500 m, Tables 1 & 2). In warm waters, radiolarian densities are highest at approximately 0 to 100 m (Boltovskoy 2017), and the contribution of deep-dwelling forms to the vertical flux is likely low (Petrushevskaya 1971b, Berger 1976). In a detailed analysis of radiolarian vertical distributions, Boltovskoy (2017) suggested that enhanced dissolution of biogenic silica in the upper traps, where the materials collected remain *in situ* for periods of up to over a year before being retrieved, may be responsible for this effect. The fact that dissolution of biogenic silica is significantly higher in the upper 1000 m, stabilizing below this depth (Berger 1968, 1976, Hurd 1972, Erez et al. 1982, Hurd & Takahashi 1983, Takahashi 1991, Abrantes et al. 2002), supports this conclusion. Lateral advection and resuspension of bottom deposits may play important roles in some areas, but are unlikely to explain this positive relationship between trap depth and radiolarian flux rates globally (see discussion in Boltovskoy 2017).

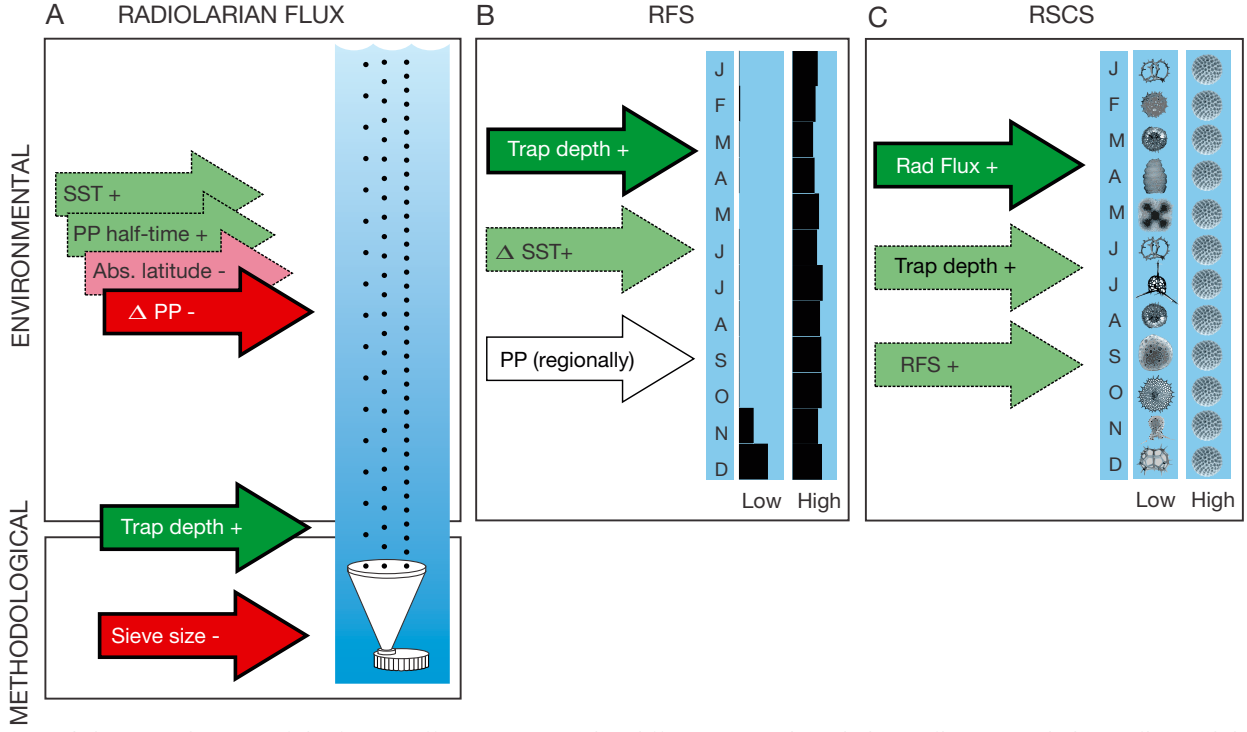


Fig. 13. Schematic diagram of the factors affecting geographic differences in (A) radiolarian flux, (B) radiolarian flux stability (RFS), and (C) radiolarian specific composition similarity (RSCS). Intensity of shading of arrows denotes the strength of the effect (dark shading, solid thick outline: strong effect; light shading, dashed outline: smaller effect). White arrow indicates the regionally variable influence of primary production (PP) on RFS, whereby in low productivity areas (and low PP half-times) RFS is lower than in medium and high PP areas. +: Positive effect; −:negative effect. Superimposed arrows denote intercorrelated independent variables. Cartoons on the right-hand side of each panel illustrate the variable discussed: (A) different flux rates into the traps, (B) different modes of total annual flux distribution throughout the year, and (C) contrasts in the radiolarian specific compositions in the traps throughout the year

Author copy

Similarity in radiolarian species compositions

RSCS is strongly affected by absolute radiolarian flux values (Figs. 7B & 13). This association may be partly influenced by the fact that specific inventories were more exhaustive in samples with more individuals, but this bias does not seem to account for the bulk of the data. For 27 of the 73 series analyzed, the original sources provided information on the specimens per sample counted and identified. Interestingly, the 5 'anomalous' series with the lowest mean sample-to-sample similarities (1 to 3, 29 and 33; Figs. 2 & 7) reported the lowest numbers of specimens identified per sample (range of means: 5 to 23), as opposed to 40 to 848 radiolarians per sample for the remaining 22 series. However, for 22 (of 27) series, sample-to-sample similarities were not affected by sample size (Spearman's $R = 0.226$, $p = 0.312$), which supports the assumption that, with the exception of a few series with extremely low sample sizes, most of the data were not biased by this effect. This result is generally in line with the fact that highest mean annual fluxes are associated with low latitude areas (Figs. 3 & 4A), where seasonal changes are less pronounced.

Previous data on temporal changes in radiolarian species compositions suggest that environmental forcing may be responsible for dominance shifts of a few species, but it does not engender massive changes in the composition of radiolarian assemblages. In the Sea of Okhotsk, some shallow-living species have been reported to peak during the spring and fall phytoplankton blooms, while several deep-living ones peak in fall only (Hays & Morley 2003). In several areas of the North Pacific and the Arctic, seasonal shifts in the dominance of a few species (e.g. *Joergensenium arcticum, Rhizoplegma boreale, Lithomelissa* sp., *Pseudocubus obeliscus*) have been associated with the input of freshwater from melting sea ice and continental runoff, brine drainage, and vertical mixing (Okazaki et al. 2003, Ikenoue et al. 2012b, 2016). *L. setosa* has also been found to show a clear seasonal productivity-related signal in the western Arctic Ocean (Ikenoue et al. 2015) and, together with *Ceratospyris borealis*, in the eastern subarctic Pacific (Takahashi 1997). Seasonal changes in the circulation around Japan have been found to affect the fluxes of a few species associated with cold (*L. setosa*) and warm water conditions (*Arachnocorallium calvata, P. obeliscus*), whereas *Cladococcus cervicornis* dominates at times of lowest radiolarian flux (Itaki et al. 2008).

Sediment trap surveys conducted in warmer-water areas also indicate a more or less marked seasonal dominance shifts of a few radiolarians, whereas the bulk of the assemblages remains roughly unchanged. In the South China Sea, the relative abundances of *Botryocyrtis scutum* and *Pterocorys hertwigii* have been associated with seasonal changes in the monsoonal circulation (Zhang et al. 2009). In the subtropical North Pacific, only 1 polycystine species (*Lithopera bacca*) has been found to react to seasonal environmental changes (Gowing 1993). In the California Current, spring upwelling has been shown to be reflected by flux changes of only 1 deep-living species, *Lithomelissa setosa* (Lange et al. 1997). In the central equatorial Pacific, only a few species (e.g. *Tetrapyle octacantha, Lophophaena hispida*) have been reported to clearly reflect changes in physical process, whereas the influence of biological forcing was concluded to be minor (Welling & Pisias 1998).

In agreement with these reports, the results of the present work suggest that major rearrangements in the specific compositions of Radiolaria at any given site are rare, and usually restricted to areas where environmental conditions undergo drastic seasonal changes. Under these settings, however, the few species that do convey a seasonal signal can represent very significant proportions of the overall assemblage (e.g. Ikenoue et al. 2015). This type of response has also been observed in several other microplanktonic organisms, including silicoflagellates, diatoms, and foraminifers (Thunell & Honjo 1987, Sancetta 1995, Marchant et al. 1998, Kincaid et al. 2000, Romero et al. 2001, 2002, Venrick et al. 2008).

An important caveat to the effects of seasonality on isolated radiolarian species is, however, that given the high diversity of the group, radiolarian inventories in any given time series of sediment trap samples range from approximately 10 to >140 species (Table 1). Thus the probabilities that 1 or a few species will show a significant correlation with any environmental trait simply by chance are high.

Another important driver of RSCS is trap depth, which yielded significant figures in the pairwise contrasts (Table 4; but not in the multivariate analysis, Table 5). This association was most clear when comparing the results of simultaneous deployments at 2 different depths, where radiolarian flux, RFS, overall species richness, and RSCS were higher in the lower than in the upper trap of each pair (Fig. 6). Several alternative or complementary mechanisms can explain this trend. Deeper traps (and areas where autotrophic production is more evenly distributed throughout the year) favor less punctuated radiolar-

Author copy

ian accumulation rates, which in turn are associated with smaller seasonal differences in radiolarian species compositions throughout the year. Enhanced dissolution of delicate species in the upper trap can also contribute to these differences (see above section), especially considering that the first sample of each series spent much more time *in situ* before being recovered than the last one. It is also conceivable that, with increasing trap depth, sharp flux pulses in the upper layers are smoothed out by mid-water biological activity (Lampitt & Antia 1997), the 'statistical funnel' from which particles are collected is larger (Siegel et al. 1990), and the input of laterally advected shells is higher (Boltovskoy 2017), resulting in temporally more homogeneous radiolarian assemblages.

Biogeographic and paleoecological implications

The results of the analyses presented indicate that seasonal environmental differences are generally poorly defined in the radiolarian flux, especially at greater depths, suggesting that seasonality of the signal preserved in the surface sediments is even less marked than that observed in the water column. For large scale biogeographic surveys and most paleoecological applications, both typically based on surface sediment samples (CLIMAP Project Members 1976, Johnson & Nigrini 1980, 1982, Cortese & Prebble 2015, Boltovskoy & Correa 2016), the fact that seasonality does not affect the sedimentary record is a welcome trait because it reinforces the assumption that specific inventories are not biased towards a restricted season characterized by extreme environmental values (e.g. Sancetta 1989, Sautter & Sancetta 1992). Further, the fact that the intermittency in radiolarian flux has a limited effect on temporal changes in their assemblages lends additional support to the use of the time-averaging sedimentary record for biogeographic and paleoceanographic surveys.

The downside, however, is that the environmental signal conveyed by radiolarian specific compositions in sediment trap samples is generally weak, especially on regional and local scales, and depends strongly on absolute radiolarian flux rates, as well as on water column depth above the trap. The latter effect is likely enhanced in the sediments, where the environmental signal of the radiolarian flux-producing layers is further modified by post-mortem mechanisms, including dissolution, reworking, lateral advection, and winnowing along the bottom by deep currents (Boltovskoy 1994).

CONCLUSIONS

(1) Radiolarian flux rates are highest in the tropics and subtropics, decreasing towards the high latitudes.

(2) At all sites where traps were deployed simultaneously at different depths, mean annual radiolarian flux rates are strongly (positively) associated with trap depth (likely a methodological artifact).

(3) In areas where primary production (PP) is low, radiolarian fluxes tend to increase in association with the short periods of enhanced productivity, whereas in areas where PP is moderate or high, their fluxes are not associated with phytoplanktonic growth cycles. Thus, geographically, associations between radiolarian flux stability (RFS) and annual PP half-times and ΔPP are weak. The fact that many polycystine species possess algal symbionts and can feed autotrophically may partly explain this decoupling between their flux rates and PP.

(4) Lowest RFS values occur in seasonally ice-covered Southern Ocean waters, yet several also seasonally ice-covered northern hemisphere sites depict variable and often high RFS values, comparable to those in the tropics and subtropics, where RFS is highest. This contrast is likely due to differences in the mechanisms that govern the production and recycling of organic matter in the upper ocean and at mid depths.

(5) Radiolarian flux rates and their species richness do not seem to be temporally coupled, but this association is obscured by the fact that, in the database analyzed, the sample sizes (i.e. numbers of radiolarians identified) of periods of high radiolarian flux are larger than those of periods with low flux. A similar bias precludes from investigating geographic associations between mean annual flux and species richness, which is further confounded by the concomitant association between lower flux rates and lower diversity at higher latitudes and lower sea surface temperatures.

(6) At any given site, temporal changes in the species composition are generally low, with the exception of the seasonally ice-covered Southern Ocean, and shallow (300 m) Sea of Okhotsk waters. Geographically, mean annual RSCS is positively associated with mean annual radiolarian flux.

(7) Comparison of simultaneous deployments at 2 different depths shows that radiolarian flux, RFS, overall species richness, and RSCS are usually higher in the lower than in the upper trap of each pair. Blurring of the near-surface seasonal signal and enhanced dissolution of delicate species in the upper trap are likely responsible for this pattern.

Author copy

(8) At any given site, seasonal variations in the radiolarian species composition affect only a few selected species, whereas the bulk of the associations remains relatively stable.

Acknowledgements. This work was partly supported by grants from the Census of Marine Zooplankton (CMarZ); a field project of the Census of Marine Life (CoML); Consejo Nacional de Investigaciones Científicas y Técnicas (Argentina); and Agencia Nacional de Promoción Científica y Tecnológica (Argentina). Four anonymous reviewers made helpful comments on an earlier version of the manuscript.

LITERATURE CITED

Abelmann A (1992) Radiolarian flux in Antarctic waters (Drake Passage, Powell Basin, Bransfield Strait). Polar Biol 12:357–372

Abrantes F, Meggers H, Nave S, Bollman J and others (2002) Fluxes of micro-organisms along a productivity gradient in the Canary Islands region (29° N). Deep-Sea Res II 49: 3599–3629

Adl SM, Simpson AG, Lane CE, Lukes J and others (2012) The revised classification of eukaryotes. J Eukaryot Microbiol 59:429–493

Anabalón V, Morales CE, González HE, Menschel E and others (2016) Micro-phytoplankton community structure in the coastal upwelling zone off Concepción (central Chile): Annual and inter-annual fluctuations in a highly dynamic environment. Prog Oceanogr 149:174–188

Arrigo KR, Perovich DK, Pickart RS, Brown ZW and others (2012) Massive phytoplankton blooms under Arctic sea ice. Science 336:1408

Asahi H, Takahashi K (2007) A 9-year time-series of planktonic foraminifer fluxes and environmental change in the Bering sea and the central subarctic Pacific Ocean, 1990–1999. Prog Oceanogr 72:343–363

Beers JR, Stewart GL (1971) Micro-zooplankton in the plankton communities of the upper waters of the eastern tropical Pacific. Deep-Sea Res Oceanogr Abst 18:861–883

Belsley DA, Kuh E, Welsch RE (1980) Regression diagnostics: identifying influential data and sources of collinearity. Wiley, New York, NY

Berger WH (1968) Radiolarian skeletons: solution at depths. Science 159:1237–1239

Berger WH (1976) Biogenous deep-sea sediments: production, preservation and interpretation. In: Riley JP, Chichester R (eds) Chemical oceanography. Academic Press, London, p 265–388

Berger WH, Wefer G (1990) Export production: seasonality and intermittency, and paleoceanographic implications. Palaeogeogr Palaeoclimatol Palaeoecol 89:245–254

Bjørklund KR (1972) Radiolarienes (Rhizopoda, Protozoa) arvariasjon og vertikalfordeling i Korsfjorden, Vest Norge, med bemerkninger om de vanligste artenes systematikk og geografiske utbredelse. PhD thesis, University of Bergen

Bjørklund KR (1974) The seasonal occurrence and depth zonation of radiolarians in Korsfjorden, Western Norway. Sarsia 56:13–42

Bolton HC (1991) On the mathematical significance of the similarity index of Ochiai as a measure for biogeographical habitats. Aust J Zool 39:143–156

Boltovskoy D (1994) The sedimentary record of pelagic biogeography. Prog Oceanogr 34:135–160

Boltovskoy D (2017) Vertical distribution patterns of Radiolaria Polycystina (Protista) in the World Ocean: living ranges, isothermal submersion, and settling shells. J Plankton Res 39:330–349

Boltovskoy D, Alder VA (1992a) Microzooplankton and tintinnid species-specific assemblage structures: patterns of distribution and year-to-year variations in the Weddell Sea (Antarctica). J Plankton Res 14:1405–1423

Boltovskoy D, Alder VA (1992b) Paleoecological implications of radiolarian distribution and standing stocks vs. accumulation rates in the Weddell Sea. In: Kennett JP, Warnke DA (eds) The Antarctic paleoenvironment: a perspective on global change: part 1. American Geophysical Union, Washington, DC, p 377–384

Boltovskoy D, Correa N (2016) Biogeography of Radiolaria Polycystina (Protista) in the World Ocean. Prog Oceanogr 149:82–105

Boltovskoy D, Correa N (2017) Planktonic equatorial diversity troughs: fact or artifact? Latitudinal diversity gradients in Radiolaria. Ecology 98:112–124

Boltovskoy D, Riedel WR (1987) Polycystine Radiolaria of the California Current region: seasonal and geographic patterns. Mar Micropaleontol 12:65–104

Boltovskoy D, Alder VA, Abelmann A (1993) Annual flux of Radiolaria and other shelled plankters in the eastern equatorial Atlantic at 853 m: seasonal variations and polycystine species-specific responses. Deep-Sea Res I 40:1863–1895

Boltovskoy D, Uliana E, Wefer G (1996) Seasonal variations in the flux of microplankton and radiolarian assemblage compositions in the northeastern tropical Atlantic at 2195 m. Limnol Oceanogr 41:615–635

Boltovskoy D, Kling SA, Takahashi K, Bjørklund K (2010) World atlas of distribution of Recent Polycystina (Radiolaria). Palaeontol Electronica 13:1–229

Boyer TP, Antonov JI, Baranova OK, Coleman C and others (2013) World Ocean Database 2013. Levitus S, Mishonov A (eds) NOAA Atlas NESDIS 72. NOAA, Silver Spring

Brown CW, Schollaert Uz S, Corliss BH (2014) Seasonality of oceanic primary production and its interannual variability from 1998 to 2007. Deep-Sea Res I 90:166–175

Caron DA, Swanberg NR (1990) The ecology of planktonic sarcodines. Aquat Sci 3:147–180

CLIMAP Project Members (1976) The surface of the ice-age Earth. Science 191:1131–1137

Cortese G, Prebble J (2015) A radiolarian-based modern analogue dataset for palaeoenvironmental reconstructions in the southwest Pacific. Mar Micropaleontol 118: 34–49

Cortese G, Bjørklund KR, Dolven JK (2003) Polycystine radiolarians in the Greenland–Iceland–Norwegian Seas: species and assemblage distribution. Sarsia 88:65–88

De Wever P, Dumitrica P, Caulet J, Nigrini C, Caridroit M (2001) Radiolarians in the sedimentary record. Gordon and Breach, Amsterdam

Eguchi NO, Kawahata H, Taira A (1999) Seasonal response of planktonic Foraminifera to surface ocean condition: sediment trap results from the central North Pacific Ocean. J Oceanogr 55:681–691

Erez J, Takahashi K, Honjo S (1982) *In situ* dissolution experiment of Radiolaria in the central North Pacific Ocean. Earth Planet Sci Lett 59:245–254

Author copy

Fay AR, McKinley GA (2014) Global open-ocean biomes: mean and temporal variability. Earth Syst Sci Data 6: 273–284

Gowing MM (1993) Seasonal radiolarian flux at the VERTEX North Pacific time-series site. Deep-Sea Res I 40: 517–545

Hammer Ø, Harper DAT, Ryan PD (2001) PAST: Paleontological statistics software package for education and data analysis. Palaeontol Electronica 4:1–9

Hays JD, Morley JJ (2003) The Sea of Okhotsk: a window on the Ice Age Ocean. Deep-Sea Res I 50:1481–1506

Hubálek Z (1982) Coefficients of association and similarity, based on binary (presence-absence) data: an evaluation. Biol Rev Camb Philos Soc 57:669–689

Hurd DC (1972) Factors affecting solution rate of biogenic opal in seawater. Earth Planet Sci Lett 15:411–417

Hurd DC, Takahashi K (1983) On the estimation of minimum mechanical loss during an *in situ* biogenic silica dissolution experiment. Mar Micropaleontol 7:441–447

Ikenoue T, Takahashi K, Tanaka S (2012a) Fifteen year time-series of radiolarian fluxes and environmental conditions in the Bering Sea and the central subarctic Pacific, 1990–2005. Deep-Sea Res II 61-64:17–49

Ikenoue T, Ueno H, Takahashi K (2012b) *Rhizoplegma boreale* (Radiolaria): a tracer for mesoscale eddies from coastal areas. J Geophys Res 117:C04001

Ikenoue T, Bjørklund KR, Kruglikova SB, Onodera J, Kimoto K, Harada N (2015) Flux variations and vertical distributions of siliceous Rhizaria (Radiolaria and Phaeodaria) in the western Arctic Ocean: indices of environmental changes. Biogeosciences 12:2019–2046

Ikenoue T, Bjørklund KR, Dumitrica P, Krabberød AK, Kimoto K, Matsuno K, Harada N (2016) Two new living Entactinaria (Radiolaria) species from the Arctic province: *Joergensenium arcticum* n. sp. and *Joergensenium clevei* n. sp. Mar Micropaleontol 124:75–94

Itaki T, Minoshima K, Kawahata H (2008) Radiolarian flux at an IMAGES site at the western margin of the subarctic Pacific and its seasonal relationship to the Oyashio Cold and Tsugaru Warm currents. Mar Geol 255:131–148

Johnson DA, Nigrini C (1980) Radiolaria biogeography in surface sediments of the western Indian Ocean. Mar Micropaleontol 5:111–152

Johnson DA, Nigrini C (1982) Radiolaria biogeography in surface sediments of the eastern Indian Ocean. Mar Micropaleontol 7:237–281

Kincaid E, Thunell RC, Le J, Lange CB, Weinheimer AL, Reid FMH (2000) Planktonic foraminiferal fluxes in the Santa Barbara Basin: response to seasonal and interannual hydrographic changes. Deep-Sea Res II 47: 1157–1176

King A, Howard W (2001) Seasonality of foraminiferal flux in sediment traps at Chatham Rise, SW Pacific: implications for paleotemperature estimates. Deep-Sea Res I 48: 1687–1708

King A, Howard W (2003) Planktonic foraminiferal flux seasonality in Subantarctic sediment traps: A test for paleoclimate reconstructions. Paleoceanography 18:1019

Lalande C, Nöthig EM, Somavilla R, Bauerfeind E, Shevchenko V, Okolodkov Y (2014) Variability in under-ice export fluxes of biogenic matter in the Arctic Ocean. Global Biogeochem Cycles 28:571–583

Lampitt RS, Antia AN (1997) Particle flux in deep seas: regional characteristics and temporal variability. Deep-Sea Res I 44:1377–1403

Lampitt RS, Salter I, Johns D (2009) Radiolaria: Major exporters of organic carbon to the deep ocean. Global Biogeochem Cycles 23:GB1010

Lange CB, Weinheimer AL, Reid FMH, Thunell RC (1997) Sedimentation patterns of diatoms, radiolarians and silicoflagellates in Santa Barbara Basin, California. CalCOFI Rep 38:161–170

Lazarus D, Suzuki N, Caulet JP, Nigrini C and others (2015) An evaluated list of Cenozoic-Recent radiolarian species names (Polycystinea), based on those used in the DSDP, ODP and IODP deep-sea drilling programs. Zootaxa 3999:301–333

Lima ID, Lam PJ, Doney SC (2014) Dynamics of particulate organic carbon flux in a global ocean model. Biogeosciences 11:1177–1198

Lutz MJ, Caldeira K, Dunbar RB, Behrenfeld MJ (2007) Seasonal rhythms of net primary production and particulate organic carbon flux to depth describe the efficiency of biological pump in the global ocean. J Geophys Res Oceans 112:C10011

Marchant M, Hebbeln D, Wefer G (1998) Seasonal flux patterns of planktic foraminifera in the Peru–Chile current. Deep-Sea Res I 45:1161–1185

Moore TC (1978) The distribution of radiolarian assemblages in the modern and ice-age Pacific. Mar Micropaleontol 3:229–266

Motoyama I, Ota M, Kokushou T, Tanaka Y (2005) Seasonal changes in fluxes and assemblages of radiolarians collected by sediment trap experiments in the northwestern Pacific: a family-level analysis. J Geol Soc Jpn 111: 404–416 (in Japanese with English Abstract)

Nigrini CA (1967) Radiolaria in pelagic sediments from the Indian and Atlantic Oceans. Bull Scripps Inst Oceanogr Univ Calif 11

Nigrini CA, Moore TC (1979) A guide to modern Radiolaria. Cushman Foundation for Foraminiferal Research, Special Publication 16, Washington, DC

Okazaki Y, Takahashi K, Yoshitani H, Nakatsuka T, Ikehara M, Wakatsuchi M (2003) Radiolarians under the seasonally sea-ice covered conditions in the Okhotsk Sea: flux and their implications for paleoceanography. Mar Micropaleontol 49:195–230

Okazaki Y, Takahashi K, Onodera J, Honda MC (2005) Temporal and spatial flux changes of radiolarians in the northwestern Pacific Ocean during 1997–2000. Deep-Sea Res II 52:2240–2274

Okazaki Y, Takahashi K, Asahi H (2008) Temporal fluxes of radiolarians along the W-E transect in the central and western equatorial Pacific, 1999-2002. Micropaleontology 54:71–86

Petrushevskaya MG (1971a) Radiolyarii Nassellaria v planktone Mirovogo Okeana [Radiolaria Nassellaria in the plankton of the World Ocean], Vol 9 (17). Nauka, Leningrad

Petrushevskaya MG (1971b) Spumellarian and Nassellarian Radiolaria in the plankton and bottom sediments of the Central Pacific. In: Funnel BM, Riedel WR (eds) The micropaleontology of oceans. Cambridge University Press, Cambridge, p 309–317

Pisias NG, Roelofs A, Weber M (1997) Radiolarian-based transfer functions for estimating mean surface ocean temperatures and seasonal range. Paleoceanography 12:365–379

Rangel TF, Diniz-Filho JAF, Bini LM (2010) SAM: a comprehensive application for Spatial Analysis in Macroecology. Ecography 33:46–50

Author copy

Romero OE, Hebbeln D, Wefer G (2001) Temporal and spatial variability in export production in the SE Pacific Ocean: evidence from siliceous plankton fluxes and surface sediment assemblages. Deep-Sea Res I 48:2673–2697

Romero OE, Lange CB, Wefer G (2002) Interannual variability (1988–1991) of siliceous phytoplankton fluxes off northwest Africa. J Plankton Res 24:1035–1046

Sancetta C (1989) Processes controlling the accumulation of diatoms in sediments: a model derived from British Columbian fjords. Paleoceanography 4:235–251

Sancetta C (1995) Diatoms in the Gulf of California: seasonal flux patterns and the sediment record for the last 15,000 years. Paleoceanography 10:67–84

Sautter Rl, Sancetta C (1992) Seasonal associations of phytoplankton and planktic foraminifera in an upwelling region and their contribution to the seafloor. Mar Micropaleontol 18:263–279

Schröder-Ritzrau A (1995) Aktuopaläontologische Untersuchung zu Verbreitung und Vertikalfluß von Radiolarien sowie ihre räumliche und zeitliche Entwicklung im Europäischen Nordmeer. PhD thesis, Christian Albrechts Universität, Kiel

Siegel DA, Granata TC, Michaels F, Dickey TD (1990) Mesoscale eddy diffusion, particle sinking, and the interpretation of sediment trap data. J Geophys Res 95:5305–5311

Smetacek V, Scharek R, Nöthig M (1990) Seasonal and regional variation in the pelagial and its relationship to the life history cycle of krill. In: Kerry KR, Hempel G (eds) Antarctic ecosystems. Ecological change and conservation. Springer, Berlin, p 103–114

Strelkov AA, Reshetnjak VV (1971) Koloniyalnie radiolyarii Spumellaria mirovogo okeana [Colonial radiolarians Spumellaria of the World Ocean], Vol IX (XVII). Nauka, Moscow

Suzuki N, Not F (2015) Biology and ecology of Radiolaria. In: Ohtsuka S, Suzaki T, Horiguchi T, Suzuki N, Not F (eds) Marine protists. Diversity and dynamics. Springer, Tokyo, p 179–222

Takahashi K (1987) Radiolarian flux and seasonality: climatic and El Niño response in the Subarctic Pacific, 1982–1984. Global Biogeochem Cycles 1:213–231

Takahashi K (1991) Radiolaria: flux, ecology, and taxonomy in the Pacific and Atlantic. Ocean Biocoenosis Series 3. WHOI, Woods Hole, MA

Takahashi K (1997) Time-series fluxes of Radiolaria in the eastern subarctic Pacific Ocean. News Osaka Micropaleontol Spec Vol 10:299–309

Takahashi K, Yamashita H (2004) Temporal and vertical flux changes in the western and central equatorial Pacific during the 1999 La Niña conditions. J Geol Soc Jpn 110: 463–479 (in Japanese with English Abstract)

Thunell RC, Honjo S (1987) Seasonal and interannual changes in planktonic foraminiferal production in the North Pacific. Nature 328:335–337

Venrick EL, Reid FMH, Weinheimer A, Lange CB, Dever EP (2006) Temporal patterns of siliceous flux in the Santa Barbara basin: the influence of North Pacific and local oceanographic processes. CCOFI Rep 47: 156–173

Venrick EL, Lange CB, Reid FMH, Dever EP (2008) Temporal patterns of species composition of siliceous phytoplankton flux in the Santa Barbara Basin. J Plankton Res 30:283–297

Welling LA, Pisias NG (1998) Radiolarian fluxes, stocks, and population residence times in surface waters of the Central Equatorial Pacific. Deep-Sea Res I 45:639–671

Wolda H (1981) Similarity indices, sample size and diversity. Oecologia 50:296–302

Zhang L, Chen M, Xiang R, Zhang J, Liu C, Huang L, Lu J (2009) Distribution of polycystine radiolarians in the northern South China Sea in September 2005. Mar Micropaleontol 70:20–38

Editorial responsibility: Marsh Youngbluth, Fort Pierce, Florida, USA

Submitted: February 13, 2017; Accepted: June 18, 2017
Proofs received from author(s): August 12, 2017